

Development of a Novel Genetically Encoded FRET System Using the Unnatural Amino Acid Anap

Author: Amanda Mitchell

Persistent link: <http://hdl.handle.net/2345/bc-ir:107177>

This work is posted on [eScholarship@BC](#),
Boston College University Libraries.

Boston College Electronic Thesis or Dissertation, 2016

Copyright is held by the author. This work is licensed under a Creative Commons Attribution-NoDerivatives 4.0 International License (<http://creativecommons.org/licenses/by-nd/4.0>).

DEVELOPMENT OF A NOVEL
GENETICALLY ENCODED FRET SYSTEM
USING THE UNNATURAL AMINO ACID
ANAP

by

AMANDA MITCHELL

A thesis submitted to the Faculty of
the department of Chemistry
in partial fulfillment
of the requirements for the degree of
Master of Science
August 2016

Boston College
Morrissey College of Arts and Sciences
Graduate School

DEVELOPMENT OF A NOVEL GENETICALLY ENCODED FRET SYSTEM USING THE UNNATURAL AMINO ACID ANAP

Amanda Mitchell

Thesis advisor: Professor Abhishek Chatterjee, Ph.D.

Abstract

Förster Resonance Energy Transfer (FRET) offers a powerful approach to study biomolecular dynamics *in vitro* as well as *in vivo*. The ability to apply FRET imaging to proteins in living cells provides an excellent tool to monitor important dynamic events such as protein conformational changes, protein-protein interactions, and proteolysis reactions. However, selectively incorporating two distinct fluorophores into the target protein(s) that are capable of FRET interaction within the complex cellular milieu is challenging. Consequently, terminal fusion to genetically encoded fluorescent proteins has emerged as the predominant labeling strategy for FRET studies *in vivo*. However, a major limitation of this strategy stems from the large size of the fluorescent proteins, which may perturb the native properties of the target, and restricted attachment only to the termini of the target. We reasoned that using genetically encoded fluorescent unnatural amino acids would overcome several of these challenges associated with currently available labeling strategies owing to their small size and the ability to introduce them site-

specifically and co-translationally. Here, we report the use of the fluorescent unnatural amino acid “Anap” as a FRET donor with green and yellow fluorescent protein acceptors. We demonstrate the utility of this labeling strategy using proteolysis and conformational change models, and step towards *in vivo* studies by further developing a proteolysis system in cell lysates.

Dedication

To my son William Mitchell

Acknowledgements

I first would like to thank my research advisor, Dr. Abhishek Chatterjee for teaching me all of the research skills I have learned at Boston College. I truly appreciate his patience in helping me these past few years.

I would also like to thank my family, especially my husband Ted and son William. Ted, you have been the most amazing and supportive husband I could ask for, and all of the weekends in the lab would have been lonely without you. William, in your short life so far you have taught me so much about being the best person I can be. You're amazement in life's little blessings is such a wonderful lesson in finding happiness in simplicity.

To the rest of my family, I thank you for all your help and motivation, especially with the distance between us. You've all bent over backwards to make my life so great.

Finally, I would like to thank my fellow lab members for their help and support in these past few hectic years. Yunan, you are a great group leader! Keep up the good work. Partha, and Melissa-I don't know how I will ever thank you enough for lending me your amazing helping hands. You have become great friends!

List of Abbreviations

UAA	unnatural amino acid
SPPS	solid phase peptide synthesis
aaRS	aminoacyl tRNA synthetase
EF-Tu	elongation factor Tu
RF	release factor
FRET	Förster resonance energy transfer
ASBT	acceptor spectral bleed through
DSBT	donor spectral bleed through
FP	fluorescent protein
QD	quantum dot
LLL	luminescent lanthanide label
PRIME	probe incorporation mediated by enzymes
AGT	O ⁶ -alkylguanine transferase
EDT	ethanedithiol
FlAsH	fluorescein arsenical hairpin binder
ReAsH	resorufin arsenical hairpin binder
EGFP	Enhanced Green Fluorescent Protein
SUMO*	Small Ubiquitin-like Modifier

Table of Contents

Chapter 1. Introduction to Genetically Encoded Unnatural Amino Acids	1
Methods of UAA incorporation into proteins	2
Genetic UAA incorporation into proteins with evolved tRNA/aaRS	2
The UAA Anap	4
Research scope	4
References	6
Chapter 2. Introduction to FRET	7
Overview of the FRET phenomenon	8
Quantifying FRET	11
Fluorophore labeling strategies: Fluorescent proteins	13
Fluorophore labeling strategies: Self-labeling proteins	16
Fluorophore labeling strategies: Peptide labels	17
Fluorophore labeling strategies: Tetracysteine labels	18
Fluorophore labeling strategies: Genetically encoded UAAs	20
References	21
Chapter 3. The Anap-EGFP FRET pair	23
Abstract	24
Introduction	25
Results	28
Discussion	38
Materials and Methods	41
References	45

Chapter 4. Optimization of the FP FRET Partner for Anap	47
Abstract	48
Introduction	49
Results	50
Discussion	56
Materials and Methods	60
References	64
Chapter 5. Future Directions	65
References	70
Appendix 1. Supporting information	71

List of Figures

- Fig 1.1 Structure of Anap
- Fig 2.1 Jablonski diagram for a single molecule
- Fig 2.2 Jablonski diagram for FRET between two molecules
- Fig 2.3 FRET efficiency curve
- Fig 2.4 Spectral overlap required for FRET
- Fig 2.5 Different methods for labeling proteins with organic fluorophores
- Fig 3.1 Model systems used in the Anap-EGFP FRET studies
- Fig 3.2 Fluorescence of EGFP-Y39Anap before and after linearization
- Fig 3.3 Fluorescence of EGFPwt versus EGFP-Y39Anap with 365 nm excitation
- Fig 3.4 Relative quantum yield of Anap in water
- Fig 3.5 Proteolysis of SUMO* constructs containing the Anap-EGFP FRET pair
- Fig 3.6 Conformational change of calmodulin constructs containing the Anap-EGFP FRET pair
- Fig 3.7 FRET ratios of calmodulin mutants with Anap-EGFP FRET pair
- Fig 4.1 *In vitro* SUMO* cleavage of SUMO*(E52Anap)-YFP systems
- Fig 4.2 *In vitro* cleavage of SUMO*(E52Anap)-DEVD-YFP systems with caspase-3
- Fig 4.3 SUMO*(E52Anap)-DEVD-YPet cleavage in cell lysates
- Fig 5.1 Incorporation of dansylalanine (Dan) into EGFP-TAG39 protein HEK293 cells

**Chapter 1: Introduction to Genetically Encoded Unnatural Amino
Acids**

The ability to site-specifically incorporate unnatural amino acids into proteins provide a powerful approach to understand, change, and enhance protein structure and function.^{1,2} By incorporating UAAs with chemistries that the 20 canonical amino acids lack, we have the ability to develop proteins with enhanced or modified biological, physiochemical, or even pharmacological properties. A variety of methods such as solid phase peptide synthesis (SPPS)³ and native chemical ligation,⁴ have been used to accomplish UAA incorporation into proteins. However, these techniques have limitations such as the inability to be used intracellularly, the need for protecting groups, and constraints on protein folding and size.^{1, 5}

A different approach to incorporating UAAs into proteins is to co-translationally incorporate the UAA of interest into the target protein. Several methods have been developed to accomplish this. For example, in one method a chemically aminoacylated tRNA was used to deliver an UAA of interest in response to a nonsense codon in a cell-free translation system.⁶ Chemically aminoacylated tRNAs were also microinjected into living cells to participate in cellular protein biosynthesis.⁷ However, these methods are technically challenging and can require stoichiometric amounts unstable aminoacyl-tRNAs; because the tRNAs require chemical acylation, they can not be recycled inside the cell.

A better approach of genetic site-specific UAA incorporation into proteins is to model the system evolved by living cells in which an orthogonal set of iso-tRNAs and aminoacyl-tRNA synthetases (aaRSs) exist for each of the 20 canonical amino acids. The aaRS “charges” (aminoacylates) the appropriate tRNA with the proper amino acid. Elongation factor Tu (EF-Tu) generally recognizes charged tRNAs and

transports them to the ribosome. In the ribosome, base pairing between the mRNA codon and the tRNA anticodon dictates the next amino acid to be added to the growing polypeptide chain. This continues as the ribosome moves along the mRNA until eventually the ribosome reaches the end of the mRNA and release factors (RF's) recognize the terminal stop codon in the mRNA. RF binding causes dissociation of the ribosomal complex and thus ends translation.¹

Of the molecular recognition events mentioned above, the steps involving tRNA aminoacylation by the aaRS and codon-anticodon base pairing are important to the site-specificity of amino acid incorporation. It follows that the key to site-specifically incorporating a new UAA is to develop a new orthogonal tRNA-aaRS pair for the UAA that can still exploit the translational machinery mentioned above.

For such a system to work, criteria involving the codon, tRNA, aaRS, and UAA must be met.⁸ First, a unique "blank" (not already coding for an aa) codon must be used and the corresponding anticodon incorporated into the tRNA. This codon must not be recognized by any of the endogenous tRNAs. Second, the new tRNA/aaRS must have no cross-reactivity; it must charge the UAA but none of the 20 canonical aa's. Finally, the UAA must be stable, available but non-toxic to the cell, tolerated by EF-Tu and the ribosome, and should not be a substrate for any of the endogenous tRNA/aaRS pairs.

Once the tRNA/aaRS pair has been evolved, one simply expresses them along with a gene containing the appropriate nonsense codon at the site of interest into cells in the presence of the UAA. The cells produce the protein containing the UAA while being grown under normal conditions. This has led to the incorporation of

over 70 UAAs with a variety of chemistries unique to the proteome into proteins using various evolved tRNA/aaRS pairs.¹ UAAs have now been used as probes for a variety of biological phenomena such as protein structure and function and protein-protein interactions.⁹

The *E. coli* Leucyl tRNA/aaRS pair was evolved in yeast to genetically encode the fluorescent UAA 3-(6-acetylnaphthalen-2-ylamino)-2-aminopropanoic acid (“Anap”) in yeast (Figure 1.1).¹⁰ This was further adapted for use in mammalian cells.¹⁵ The amino acid is fluorescent (365 nm ex, 490 nm em in water), and can be used to monitor the subcellular localization of target proteins in live mammalian cells.

The goal of the current work is to develop a new application for Anap for monitoring dynamic changes of target proteins in living cells. Here, we incorporate Anap into proteins as a Förster Resonance Energy Transfer (FRET) partner using the site-specific genetic method of incorporation of UAAs discussed above with the tRNA/AnapRS system developed for use in mammalian cells.¹¹ The following chapter discusses FRET theory and the benefits to using genetic incorporation of UAAs for FRET. The focus then turns to the development of a new FRET pair containing Anap and the model systems in which the new FRET pair has been tested. The final points of discussion are optimization of a FRET partner for Anap and continuing work.

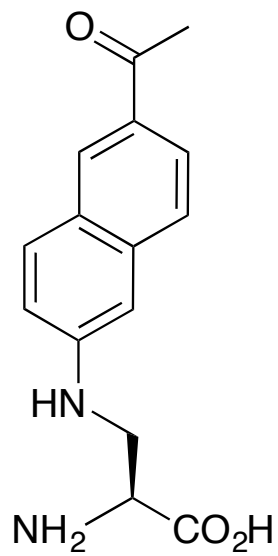


Figure 1.1 Structure of the UAA “Anap.” Anap is genetically incorporated into proteins using a Leucyl-derived tRNA/AnapRS system.¹⁰⁻¹¹

References

- (1) Liu, C. C.; Schultz, P. G. *Annu. Rev. Biochem.* **2010**, *79*, 413-444.
- (2) Xie, J.; Schultz, P. *Methods* **2005**, *36*, 227-238.
- (3) Rogers, J. M. G.; Lippert, L. G.; Gai, F. *Anal. Biochem.* **2010**, *399*, 182-189.
- (4) Hellstrand, E.; Kukora, S.; Shuman, C. F.; Steenbergen, S.; Thulin, E.; Kohli, A.; Krouse, B.; Linse, S.; Akerfeldt, K. S. *Febs J.* **2013**, *280*, 2675-2687.
- (5) Wang, L.; Schultz, P. *Angew. Chem. -Int. Edit.* **2005**, *44*, 34-66.
- (6) Noren, C.; Anthonycahill, S.; Griffith, M.; Schultz, P. *Science* **1989**, *244*, 182-188.
- (7) Rodriguez, E.; Lester, H.; Dougherty, D. *Proc. Natl. Acad. Sci. U. S. A.* **2006**, *103*, 8650-8655.
- (8) Jianming Xie, P. S. *Nature Reviews Molecular Cell Biology* **2006**, *7*, 775.
- (13-9) Davis, L.; Chin, J. W. *Nat. Rev. Mol. Cell Biol.* **2012**, *13*, 168-182.
- (10) Lee, H. S.; Guo, J.; Lemke, E. A.; Dimla, R. D.; Schultz, P. G. *J. Am. Chem. Soc.* **2009**, *131*, 12921.
- (11) Chatterjee, A.; Guo, J.; Lee, H. S.; Schultz, P. G. *J. Am. Chem. Soc.* **2013**, *135*, 12540-12543.

Chapter 2: Introduction to FRET

In recent years, the use of fluorescent reporters to study biomolecular phenomena has become commonplace in many research labs due to the noninvasive and easily accessible nature of fluorophores as well as safety. A Jablonski diagram best illustrates the fluorescence phenomenon (Figure 2.1). In order for fluorescence to occur, an electron in a molecule is excited from the spin-paired “singlet” S_0 to a more excited singlet state such as the S_2 state. Normally the electron will then relax to the lowest vibrational level of the S_2 state followed by a process called internal conversion where it goes from the lowest vibrational level in the S_2 to a higher vibrational energy state within the S_1 state. From here, the electron can change spin multiplicity to the “triplet” T_1 state by intersystem crossing, relax non-radiatively from S_1 or S_2 by static or dynamic/collisional quenching, or relax radiatively from S_1 or S_2 . The last of these possibilities is “fluorescence.”¹

A popular method that utilizes fluorescence to explore biomolecular dynamics is based on the phenomenon called Förster Resonance Energy Transfer (FRET). FRET is the process in which a blue-shifted “donor” fluorophore non-radiatively (without first emitting a photon) transfers its energy to a red-shifted “acceptor” fluorophore (Figure 2.2).²⁻⁴ The ability for this transfer to occur depends on several conditions: the two fluorophores must be in close proximity (normally ~1-10nm apart), the emission spectrum of the donor fluorophore must overlap with the excitation spectrum of the acceptor fluorophore, and their dipoles must be appropriately aligned.

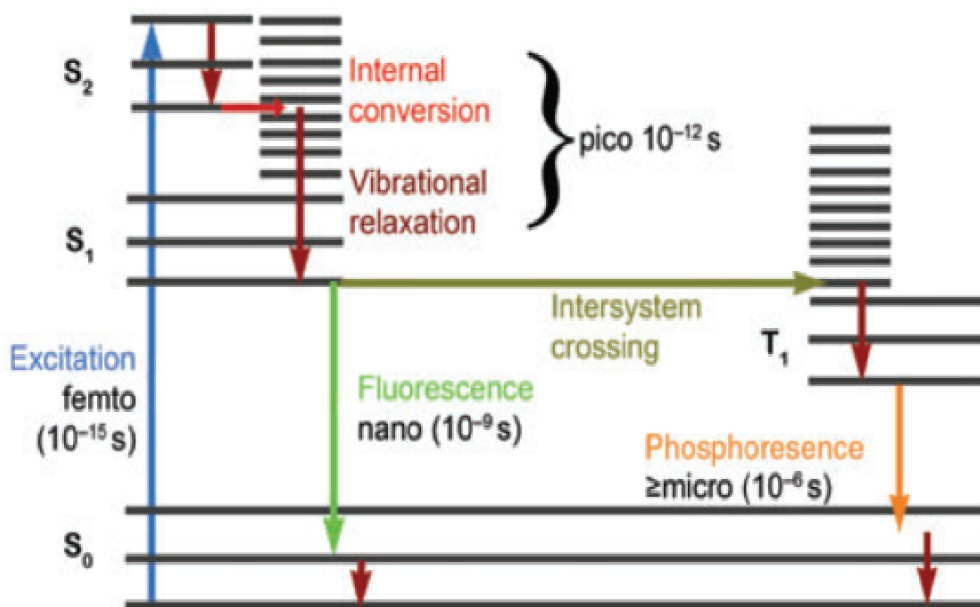


Figure 2.1⁵ Jablonski diagram for a single molecule. After electronic excitation (blue arrow) the molecule relaxes to the lowest vibrational level (dark red arrows) of S_2 excited state, undergoes internal conversion (light red arrow) in which it goes from S_2 to S_1 , allowing it to further relax vibrationally. Fluorescence (light green arrow) occurs when a photon of light is emitted from the lowest vibrational state of S_1 to the S_0 state. Fluorescence can compete with intersystem crossing (dark green arrow).

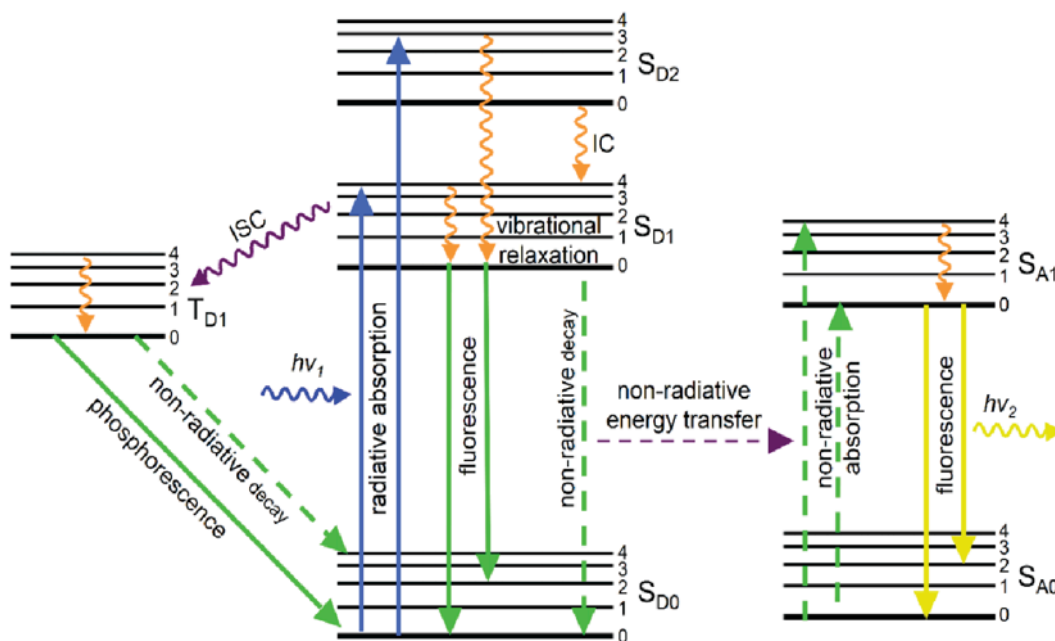


Figure 2.2⁶ Jablonski diagram for FRET between two molecules. In FRET, the energy that would normally be given off as fluorescence by the donor fluorophore is instead non-radiatively transferred to the acceptor fluorophore. The acceptor fluorophore then absorbs the energy and fluoresces. The result is that donor fluorescence decreases and acceptor fluorescence increases with FRET.

Individual FRET pairs are quantified by the FRET efficiency (E_{FRET}) and the Förster radius (R_o), which is the distance between the two fluorophores when E_{FRET} is 50% its maximal value.^{4,7,8} E_{FRET} and R_o are given by the following equations:³

$$E_{FRET} = \frac{1}{1 + \left(\frac{r}{R_o}\right)^6}$$

$$R_o(nm) = [2.8 * 10^{17} * \kappa^2 * Q_D * E_A * J(\lambda)]^{\frac{1}{6}}$$

where $J(\lambda) = \int F_D(\lambda) * E_A(\lambda) * \lambda^4 d\lambda$

Here, r is the distance between the two fluorophores, κ^2 represents the angle between the two fluorophore dipoles, Q_D is the quantum yield of the donor, E_A is the extinction coefficient of the acceptor at the absorbance maximum, and $J(\lambda)$ is the spectral overlap integral between the normalized donor fluorescence ($F_D(\lambda)$) and the acceptor excitation spectra ($E_A(\lambda)$). The value for κ^2 can range from 0-4, where 0 represents dipoles that are perpendicular to each other and 4 represents parallel dipoles. Because κ^2 is not determined experimentally, a value of 2/3, which corresponds to the average of all possible values, is normally used.

Because E_{FRET} depends on the sixth power of distance between two fluorophores, FRET is highly sensitive to changes in distance between the two fluorophores. A FRET efficiency curve shows that the sensitivity is closest at distances near R_o (the inflection point in the curve), where a small change in

distance results in a large change in E_{FRET} (Figure 2.3). On the other hand, large changes in distance are required to elicit any noticeable change in E_{FRET} at distances less than $0.5 R_0$ or greater than $1.5R_0$.⁸ As a result, FRET can be used as a molecular ruler at distances close to R_0 .

In order to design highly efficient FRET pairs, the donor should have high quantum yield and the acceptor should have a large extinction coefficient. In addition, there should be at least 30% overlap between the donor excitation spectrum and the acceptor emission spectrum.⁴ However, there should be as little overlap as possible between the excitation spectra of the donor and acceptor as well as between the emission spectra between the donor and acceptor. If the excitation spectra are not spectrally separated, then direct excitation of the acceptor can occur upon excitation of the donor and lead to inaccurate FRET measurements. If the emission spectra are not spectrally separated then the donor emission can bleed into the acceptor channel, which also leads to inaccurate FRET measurements. These interferences with FRET measurements, called acceptor spectral bleedthrough (ASBT) and donor spectral bleedthrough (DSBT), respectively, can be challenging for obtaining accurate FRET data (Figure 2.4), particularly when doing FRET microscopy. Fortunately, there are several ways to reduce or eliminate SBT, such as acceptor photobleaching and spectral unmixing.⁷

A plethora of different fluorophores are now available that can be used for FRET experiments. Such fluorophores include fluorescent proteins (FPs),^{2, 3, 8} covalent bioorthogonal labels,^{9,10} reversible binding bioorthogonal labels,¹¹ quantum dots (QDs),¹² and luminescent lanthanide labels (LLs).^{13, 14} Furthermore,

combinations of different types fluorophores can be used to create a multitude of donor-acceptor pairs.

A major challenge towards applying FRET to study molecular events in a living cell is labeling the target protein(s) selectively with the desired fluorophores. Because of this, FPs are the most widely used fluorophores for *in vivo* FRET, since donor and acceptor FPs can be genetically fused to the termini of the protein of interest. Due to their popularity, an expansive array of FPs with different photophysical properties have been engineered. Notable are red-shifted FPs, which are also useful for *in vivo* imaging.¹⁵ Other fluorescent proteins have also been developed to maximize characteristics such as large stokes shifts (to minimize SBT), large quantum yields, and large extinction coefficients.⁹ Finally, because the FPs are generally stable, incorporated co-translationally and have a fluorophore that matures autocatalytically, FPs are an ideal candidate for live-cell FRET imaging.

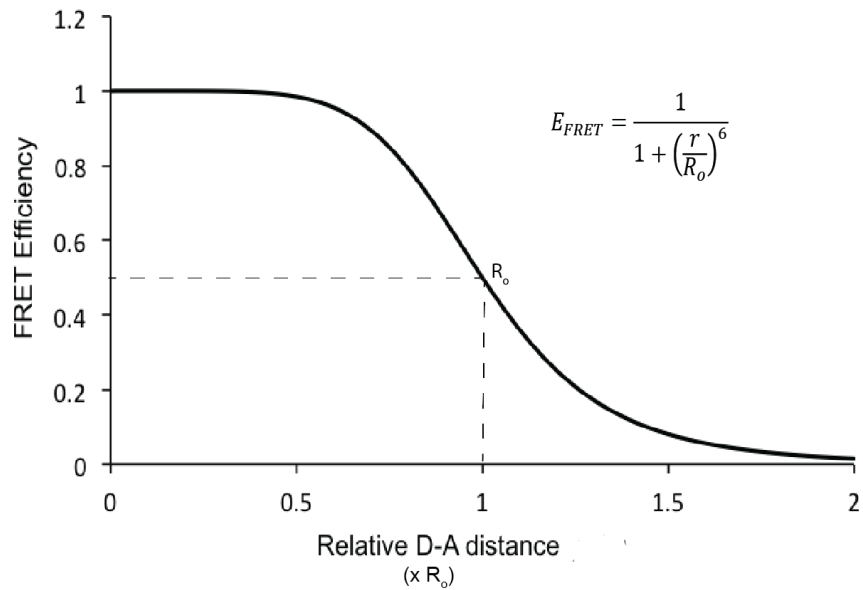


Figure 2.3 FRET efficiency curve. The FRET efficiency is high when the donor and acceptor fluorophores are close together. The FRET efficiency decreases proportionally to the sixth power as the distance between the two fluorophores increases. When FRET efficiency is 0.5, the distance between the two fluorophores is called the Förster radius (R_0). FRET efficiency is most sensitive at distances close to the Förster radius.

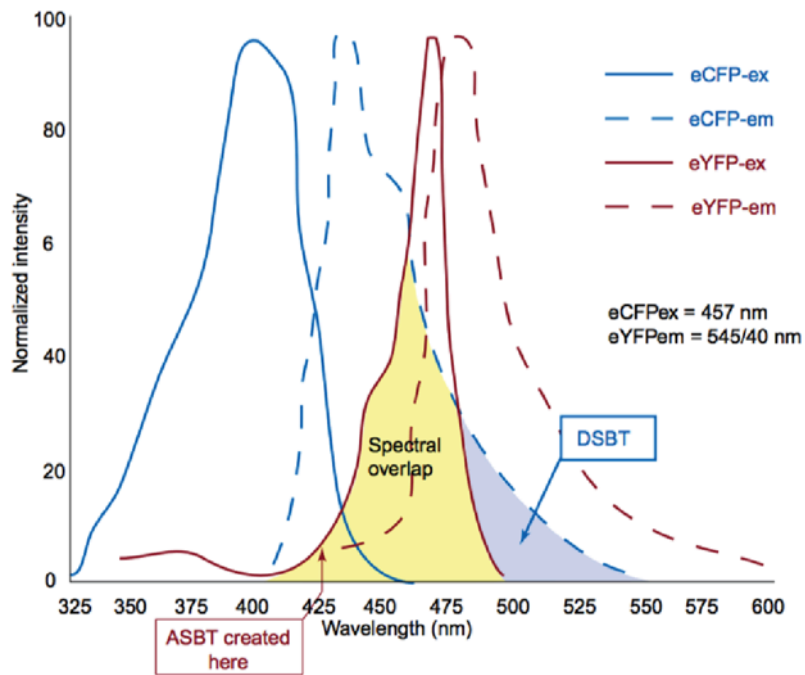


Figure 2.4⁷ Spectral overlap required for FRET. Overlap between the emission spectrum of the donor (here: eCFP) and the excitation spectrum of the acceptor (Here: eYFP) is required for FRET to occur, but overlap between the two excitation spectra (ASBT) or between the two emission spectra (DSBT) makes the quantification of FRET data more challenging.

However, the use of FPs is associated with significant limitations. One major limitation is the size, with the typical FP having a size of 23-27 kDa.⁹ This can potentially perturb the properties of the proteins under investigation. This problem is particularly exacerbated for FRET applications where two distinct FPs must be attached to the target protein(s). Additionally, attachment of FPs is largely limited to the protein termini. Again, this limitation is amplified in FRET applications where the dynamic motions under investigation may not be adequately captured by the terminal placement of the fluorescent probes. Lastly, some FPs are unstable and oligomerize.¹⁶ This can lead to the unnatural clustering of the protein to which the FPs are fused, which in turn can result in data that doesn't represent the system in its native state.^{2,3}

Another approach to attach fluorophores to a desired target protein employs protein and peptide tags that can be post-translationally modified with high selectivity. Examples of self-labeling protein tags include SNAP-tag and CLIP-tag,^{17, 18} and examples of peptide labels that can be enzymatically labeled include “probe incorporation mediated by enzymes” (PRIME) (Figure 2.5).^{18, 19} SNAP-tag and CLIP-tag work by fusing an O⁶-alkylguanine transferase (AGT) -based protein to the protein of interest. Cells are allowed to express the fusion proteins and then are incubated with the chosen fluorophore that has been tethered to either benzylguanine (for SNAP-tag) or O²-benzylcytosine (for CLIP-tag). A cysteine in the fusion SNAP-tag or CLIP-tag reacts quickly and specifically with the tethered fluorophore, leading to a benzyl-fluorophore labeled protein.⁹

A big advantage of the SNAP-tag and CLIP-tag technologies is the wide range of organic fluorophores that can be used to label the protein.¹⁸ Additionally, since SNAP-tag and CLIP-tag are specific for their substrates, they can be used simultaneously for the incorporation of different fluorophores into different molecular species.¹⁷ Finally, most SNAP-tag substrates are cell permeable, allowing protein labeling within live cells. However, the SNAP-tag and CLIP-tag technologies are not without limitations. For example, the fusion proteins in these systems have a size of ~20 kDa⁹ and therefore do not address the size concerns that exist for FPs. Finally, the use of excess probe in the post-translational labeling strategy leads to high background signal from the excess intracellular dye.

There are covalent labeling technologies that do address the size concerns brought about by the SNAP-tag and CLIP-tag systems. One such technology is PRIME. In PRIME, an engineered lipoic acid ligase or “fluorescent ligase” covalently attaches a 7-hydroxycoumarin,¹⁹ 7-aminocoumarin,²⁰ or Pacific Blue fluorophore²¹ to a 13 amino acid lipoic acid ligase acceptor peptide sequence that has been genetically incorporated onto the protein of interest.²² PRIME can be done living cells because both the enzyme and the acceptor peptide (as a fusion to the protein of interest) are expressed inside the cell and the fluorophores are membrane permeable. The acceptor peptide also only adds an additional 1.7 kDa to the protein of interest, making this the smallest size investment for fluorophore attachment so far mentioned.

One disadvantage of PRIME is that there are a limited number of fluorophores that can be added to the protein of interest due to the specificity of the

binding pocket in the engineered ligase. Furthermore, the acceptor peptide must be incorporated into the target protein such that it is accessible to the modifying enzyme but does not perturb the structure and function of the target protein. This leads to significant site-restrictions associated with the fusion of these peptides.

Another labeling strategy comes from biarsenical dyes, such as FAsH and ReAsH, that selectively bind a tetracysteine peptide tag with high affinity and selectivity.^{16, 18} These probes are introduced to cells bound to ethanedithiol (EDT) in the cell-permeable form FAsH-EDT₂, which is only weakly fluorescent on its own. The probe becomes highly fluorescent upon binding a tetracysteine motif (which displaces the EDTs). Proteins genetically fused to a Cys-Cys-Pro-Gly-Cys-Cys peptide tag can therefore be easily labeled with FAsH and ReAsH probes. These probes are also small and bind quickly. However, they are limited to reducing environments. In addition, the background from these probes tends to be high due to nonspecific binding to proteins with high cysteine content and to weak fluorescence emitted from the EDT bound probe.^{9, 18}

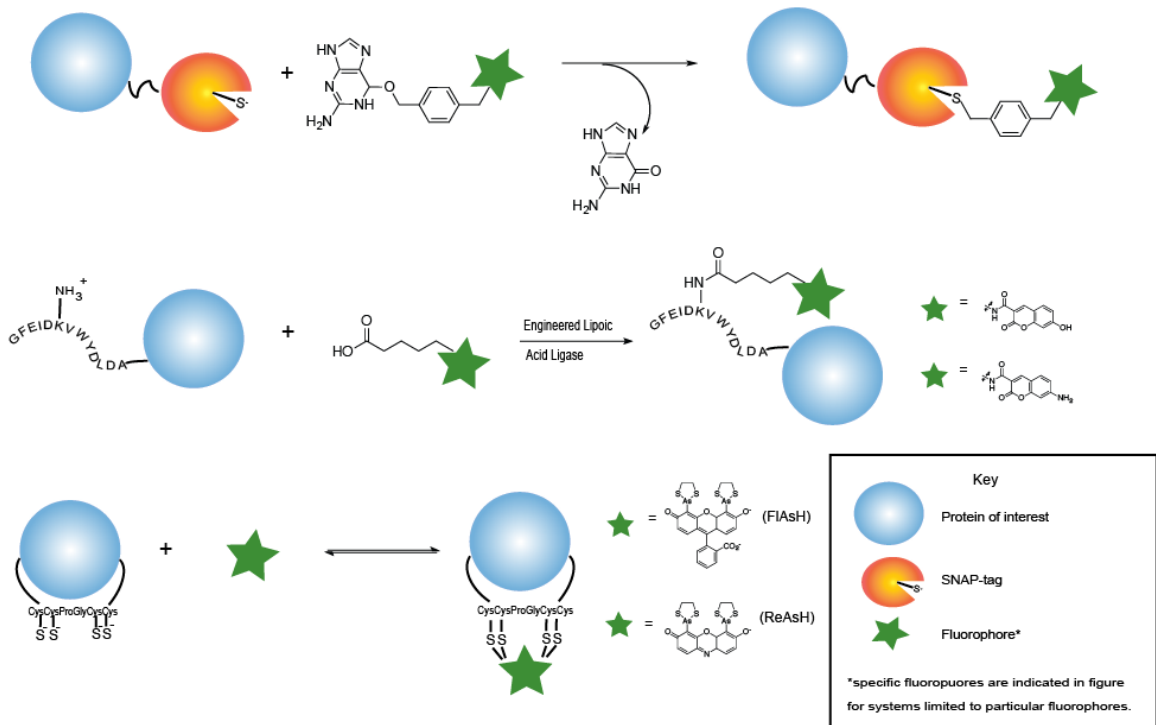


Figure 2.5 Different methods for labeling proteins with organic fluorophores. Top: in SNAP-tag labeling, an AGT fused to the protein of interest self-labels via cysteine alkylation in the presence of a benzylguanine-tethered fluorophore; CLIP-tag works similarly, but with a uses a different variant of AGT that reacts with O²-benzylcytosine tethered fluorophore. Middle: in PRIME labeling, a 13 amino acid peptide is genetically fused (either to the N- or C-terminus) to the protein of interest. An engineered lipoyl acid ligase amidates the peptide lysine with a 7-hydroxyl or 7-amino coumarin; a differently engineered lipoyl acid ligase can be used to attach a Pacific Blue fluorophore. Bottom: in FIAsh, a CCPGCC peptide motif is genetically encoded into the protein of interest. In the presence of FIAsh-EDT₂ (or ReAsh-EDT₂) in reducing environments, the probe binds FIAsh probe binds to the cysteines in the peptide motif.

We reasoned that using fluorescent UAAs incorporated into proteins by the method discussed in Chapter 1 would solve several of the issues associated with currently available labeling strategies described above. First, UAAs are small, which should minimize structural and functional perturbation to the target proteins. The small size also allows its incorporation into internal sites unlike protein or peptide fusions, which are typically restricted to termini or highly flexible loops. The UAAs are incorporated into proteins site-specifically and co-translationally which enables fluorophore labeled protein inside living cells. Moreover, since the method of UAA incorporation is general, UAAs with optimized spectral properties can be developed and a tRNA/UaaRS pair evolved for incorporation of the fluorescent probe into proteins.²⁶

Ideally, we would like to have two fluorescent UAAs site-specifically incorporated into proteins for FRET studies. However, given this technology is still at its infancy in the context of mammalian cells and fluorescent UAAs that can serve as a FRET pair in a living cell are not yet available, we set out to develop and characterize a new FRET system using the UAA Anap and a fluorescent protein. Anap, which already has an evolved tRNA/AnapRS pair,²⁷ is introduced as a FRET donor with enhanced GFP (EGFP) as a FRET acceptor in Chapter 3. The Förster radius associated with the Anap-EGFP FRET pair is also quantified, and representative *in vitro* proteolysis and conformational change studies are performed to demonstrate the utility of this new FRET pair. Chapter 4 then discusses the optimization of a FP FRET partner for Anap, and finally Chapter 5 considers the future directions for UAAs as FRET partners.

References

- (1) Lakowicz, J. In *Principles of Fluorescence Spectroscopy*; Springer: 2006; .
- (2) Hochreiter, B.; Garcia, A. P.; Schmid, J. A. *Sensors* **2015**, *15*, 26281-26314.
- (3) Piston, D. W.; Kremers, G. *Trends Biochem. Sci.* **2007**, *32*, 407-414.
- (4) Zadran, S.; Standley, S.; Wong, K.; Otiniano, E.; Amighi, A.; Baudry, M. *Appl. Microbiol. Biotechnol.* **2012**, *96*, 895-902.
- (5) Lichtman, J.; Conchello, J. *Nat. Methods* **2005**, *2*, 910-919.
- (6) Patowary, S. Protein Association in Living Cells Using FRET Spectrometry: Application to G-Protein Coupled Receptors, University of Wisconsin-Milwaukee, 2013.
- (7) Wallrabe, H.; Periasamy, A. *Curr. Opin. Biotechnol.* **2005**, *16*, 19-27.
- (8) Mueller, S.; Galliardt, H.; Schneider, J.; Barisas, B. G.; Seidel, T. *Front. Plant Sci.* **2013**, *4*, 413.
- (9) Dean, K. M.; Palmer, A. E. *Nat. Chem. Biol.* **2014**, *10*, 512-523.
- (10) Mukherjee, A.; Schroeder, C. M. *Curr. Opin. Biotechnol.* **2015**, *31*, 16-23.
- (11) Giepmans, B.; Adams, S.; Ellisman, M.; Tsien, R. *Science* **2006**, *312*, 217-224.
- (12) Resch-Genger, U.; Grabolle, M.; Cavaliere-Jaricot, S.; Nitschke, R.; Nann, T. *Nature Methods* **2008**, *5*, 763+.
- (13) de Sá, G. F.; Malta, O. L.; de Mello Donegá, C.; Simas, A. M.; Longo, R. L.; Santa-Cruz, P. A.; da Silva Jr., E. F. *Coord. Chem. Rev.* **2000**, *196*, 165-195.
- (14) Geissler, D.; Linden, S.; Liermann, K.; Wegner, K. D.; Charbonniere, L. J.; Hildebrandt, N. *Inorg. Chem.* **2014**, *53*, 1824-1838.

- (15) Lam, A. J.; St-Pierre, F.; Gong, Y.; Marshall, J. D.; Cranfill, P. J.; Baird, M. A.; McKeown, M. R.; Wiedenmann, J.; Davidson, M. W.; Schnitzer, M. J.; Tsien, R. Y.; Lin, M. Z. *Nat. Methods* **2012**, *9*, 1005-+.
- (16) Zhang, J.; Campbell, R.; Ting, A.; Tsien, R. *Nat. Rev. Mol. Cell Biol.* **2002**, *3*, 906-918.
- (17) Crivat, G.; Taraska, J. W. *Trends Biotechnol.* **2012**, *30*, 8-16.
- (18) Jing, C.; Cornish, V. W. *Acc. Chem. Res.* **2011**, *44*, 784-792.
- (19) Uttamapinant, C.; White, K. A.; Baruah, H.; Thompson, S.; Fernandez-Suarez, M.; Puthenveetil, S.; Ting, A. Y. *Proc. Natl. Acad. Sci. U. S. A.* **2010**, *107*, 10914-10919.
- (20) Jin, X.; Uttamapinant, C.; Ting, A. Y. *ChemBioChem* **2011**, *12*, 65-70.
- (21) Cohen, J. D.; Thompson, S.; Ting, A. Y. *Biochemistry (N. Y.)* **2011**, *50*, 8221-8225.
- (22) Liu, D. S.; Phipps, W. S.; Loh, K. H.; Howarth, M.; Ting, A. Y. *Acs Nano* **2012**, *6*, 11080-11087.
- (23) Uttamapinant, C.; Sanchez, M. I.; Liu, D. S.; Yao, J. Z.; Ting, A. Y. *Nature Protocols* **2013**, *8*, 1620-1634.
- (24) Thibon, A.; Pierre, V. C. *Anal. Bioanal. Chem.* **2009**, *394*, 107-120.
- (25) Rajendran, M.; Yapici, E.; Miller, L. W. *Inorg. Chem.* **2014**, *53*, 1839-1853.
- (26) Liu, C. C.; Schultz, P. G. *Annu. Rev. Biochem.* **2010**, *79*, 413-444.
- (27) Chatterjee, A.; Guo, J.; Lee, H. S.; Schultz, P. G. *J. Am. Chem. Soc.* **2013**, *135*, 12540-12543.

**Chapter 3: Development and Characterization of the Anap-EGFP
FRET Pair**

Abstract

The utility of fluorescent probes for FRET is limited by issues such as large fluorophore size and nonspecific binding. These issues can be mitigated by genetically encoding fluorescent UAAs as at least one partner of the FRET pair. We develop a genetically encoded FRET system using the UAA Anap as the FRET donor and EGFP as the FRET acceptor. Direct excitation of EGFP at the donor wavelength leads to only 11% of the EGFP emission intensity compared to FRET sensitized emission. The quantum yield of Anap in water was determined to be 0.50.

Incorporation of this data into the Förster radius calculation led to a Förster radius value of 49 Å for the Anap-EGFP FRET pair. The utility of this FRET pair to monitor dynamic changes in protein structure was demonstrated using a SUMO*-EGFP fusion protein that undergoes proteolysis in the presence of the SUMO* protease, as well as a Calmodulin-M13-EGFP fusion protein that undergoes a conformational change in the presence of calcium. The ability to introduce Anap at different positions within the target protein sequence relative to the terminally fused EGFP led to distinct spectral profiles, facilitating the optimization of the different FRET systems.

Introduction

Anap has been previously incorporated into proteins in mammalian cells using an evolved *E. coli*-derived Leucyl tRNA/aaRS.¹ Anap excites maximally around 365 nm, has a quantum yield of 0.48 in ethanol, and has an extinction coefficient of 17,500 M⁻¹ cm⁻¹. The emission spectrum of Anap is environmentally sensitive and peaks between 460-480 nm in aqueous buffer. This emission spectral window suggests that Anap may be a good FRET donor for green or yellow fluorophores that absorb in the 480-500 nm range. A FRET pair composed of Anap and a FP would be completely genetically encoded, allowing for optimal specificity of labeling, while alleviating a number of the challenges associated with FP-FP FRET pairs described earlier.

Enhanced Green Fluorescent Protein (EGFP) maximally absorbs at 488 nm with an extinction coefficient of 55,000 M⁻¹cm⁻¹, which should allow it to serve as the FRET acceptor for Anap.² EGFP is one of the first fluorescent protein developed, and is one of the most widely used FP tags, which would make the Anap-EGFP FRET pair particularly facile to adapt for the analysis of dynamic changes *in vitro* as well as *in vivo*. EGFP has also been engineered to reduce dimerization interactions,³ which is important to prevent the unnatural clustering of the protein of interest when expressed as a fusion protein.

Here we describe the development of this fully genetically encoded FRET system, using the fluorescent unnatural amino acid Anap as the donor and the EGFP as the acceptor, for application to proteins expressed in mammalian cells. The utility of this FRET pair was demonstrated by monitoring a proteolysis reaction as

well as a protein conformational change using reporter proteins expressed in mammalian cells (Figure 3.1).

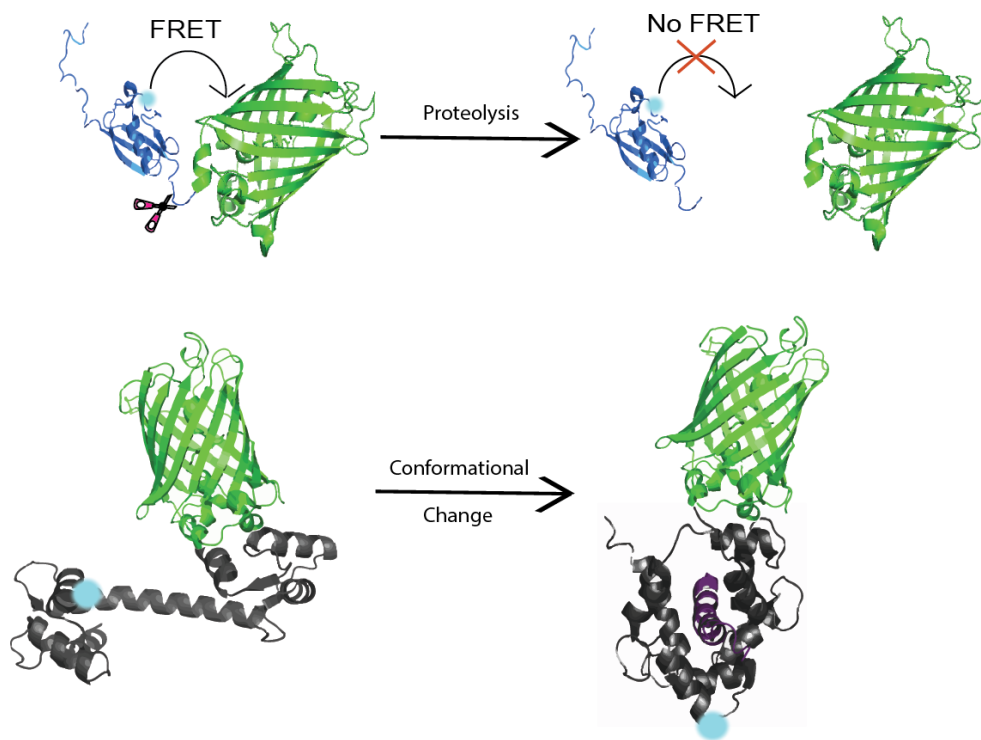


Figure 3.1 Model systems used in this study. Top: Proteolysis experiment using the Anap-incorporated SUMO* domain (blue) fused to EGFP (green). Bottom: Conformational change system using Anap-incorporated calmodulin (black) fused to the M13 peptide (purple) and EGFP.

Results

Characterization of the Anap-EGFP FRET

To determine the ability of Anap to FRET pair with EGFP, we expressed and purified EGFP-Y39Anap protein from HEK293T cells. In this mutant, the Anap residue is incorporated close to the EGFP fluorophore and should be able to participate in resonance energy transfer. We first monitored the emission spectrum of the EGFP-Y39Anap mutant with 365 nm excitation (selective excitation of the Anap fluorophore) (Figure 3.2), which closely matched the emission spectrum of EGFP and little fluorescence from Anap was observed. However, upon denaturation, the EGFP fluorescence disappeared and a large increase in Anap fluorescence was noted. Denaturing the protein abolishes the fluorescence of the EGFP fluorophore, but not Anap, and it also increases the distance between Anap and EGFP fluorophore relative to the folded state. These observations suggest successful resonance energy transfer from Anap to the EGFP fluorophore in the folded state.

To further confirm resonance energy transfer, we carefully normalized the concentrations of wild type EGFP and EGFP-Y39Anap, both expressed in HEK293T cells and purified to homogeneity, and monitored their fluorescence spectra with excitation at 365 nm (Anap) or 475 nm (EGFP). While the excitation of the EGFP fluorophore at 488 nm resulted in identical emission spectra (figure 3.3, inset), when the Anap fluorophore was excited at 365 nm, the EGFP-Y39Anap mutant exhibited significantly higher EGFP emission relative to wild-type EGFP (Figure 3.3). The emission intensity at 510 nm for EGFPwt was only 11% relative to the EGFP-Y39Anap mutant.

Calculation of Anap Quantum Yield and Anap-EGFP Förster Radius

In order to calculate the Förster radius of the Anap-EGFP FRET pair, the quantum yield of Anap in water was first calculated. This was accomplished using the relative quantum yield method. The quantum yield of Anap was calculated relative to quinine sulfate (figure 3.4, left), and quinine sulfate was cross calibrated against coumarin-1 (Figure 3.4, right). Based on slopes of the plots of fluorescence intensity over absorbance at 350 nm, the relative quantum yield of Anap in water was calculated to be 0.50. Using a quantum yield value of 0.73 for coumarin-1 in ethanol,⁴ the calculated quantum yield of quinine sulfate from cross-calibration was 0.51, a 5.8% difference compared to the accepted value of 0.54 in 0.1 M H₂SO₄.⁵ Using the quantum yield of Anap in water, the absorbance spectrum of EGFP, the emission spectrum of Anap, and the Förster radius equation (1) and overlap integral equation (2), the Förster radius of the Anap-EGFP FRET pair was determined to be 49 Å.

Monitoring a Proteolysis Reaction with the Anap-EGFP FRET Pair

Proteolysis reactions are abundant in biology and play a central role in large number of different processes.^{6,7} The ability to monitor this process *in vivo* or *in vitro* using a FRET reporter will be valuable. To evaluate if our FRET reporter is indeed useful in reporting proteolysis reactions, we designed a reporter where a Small Ubiquitin-like Modifier (SUMO*) domain was fused to the N-terminus of EGFP. This domain is cleavable with the SUMO* protease with high efficiency and

specificity, providing a great model protease cleavage reaction. Incorporation of the Anap residue within the SUMO* domain should create a FRET reporter such that upon proteolysis the distance between the Anap residue and EGFP reporter increases, which should lead to a change in the FRET emission.

Two such mutants were generated SUMO*(E52Anap)-EGFP and SUMO*(T66Anap)-EGFP, both of which can be expressed in HEK293T cells and purified to homogeneity. Cleavage of the SUMO*(E52Anap)-EGFP fusion protein with SUMO* protease was followed by fluorescence spectroscopy and SDS-PAGE (Figure 3.5, top). Before cleavage, the FRET ratio was 2.66, and after overnight incubation with the SUMO* protease, the FRET ratio was 1.21. The fluorescence image of the SDS-PAGE gel showed a complete disappearance of the fusion protein band and a new smaller band appeared corresponding to the cleaved SUMO*(E52Anap) domain.

Cleavage of SUMO*(T66Anap)-EGFP occurred more slowly than the SUMO*(E52Anap)-EGFP even in the presence of an excess amount of protease (Figure 3.5, bottom). While the binding mechanism of SUMO* protease to SUMO* domain is incompletely understood, we believe that the incorporation of the large Anap residue at this specific site (close to the cleavage site) perturbs this interaction. Before cleavage the FRET ratio was 4.12, and after overnight incubation the FRET ratio dropped to 1.50. However, after overnight incubation the fluorescence scan of the SDS-PAGE gel still showed remaining fusion protein.

These results demonstrate that proteolysis reactions can indeed be monitored using an Anap-EGFP FRET pair, and the ability to install the Anap at

variable sites into the target provides a facile approach to identify the optimal positioning.

Conformational Change Model with Cal-M13-EGFP

Protein conformational changes are ubiquitous in living systems, and the ability to monitor and control them will be valuable to our understanding of living cells.⁸ To assess the utility of our FRET system in monitoring conformational changes, we opted to design a fusion protein system of calmodulin on the N-terminus, an M13 peptide, and EGFP on the C-terminus. In the presence of Ca²⁺, calmodulin binds the M13 peptide and undergoes a conformational change. When Anap is incorporated into the calmodulin domain of this system, conformational changes induced by Ca²⁺ addition should lead to a distance change between Anap and EGFP, which should manifest itself as a change in FRET.

All of the mutants except Q136Anap had smaller FRET ratios in the presence of Ca²⁺ compared to the FRET ratios in the absence of Ca²⁺ (Figure 3.6). The FRET ratios for 0 μM Ca²⁺ were 4.1 (A47Anap), 2.4 (D51Anap), 1.6 (E55Anap), 1.8 (T80Anap), 2.7 (E88Anap), 2.6 (R91Anap) and 4.7 (Q136Anap). The FRET ratios in the presence of Ca²⁺ (25 μM) for the different mutants were 0.9 (A47Anap), 1.0 (D51Anap), 0.6 (E55Anap), 0.8 (T80Anap), 0.5 (E88Anap), 1.1 (R91Anap), and 4.8 (Q136Anap) (Figure 3.7).

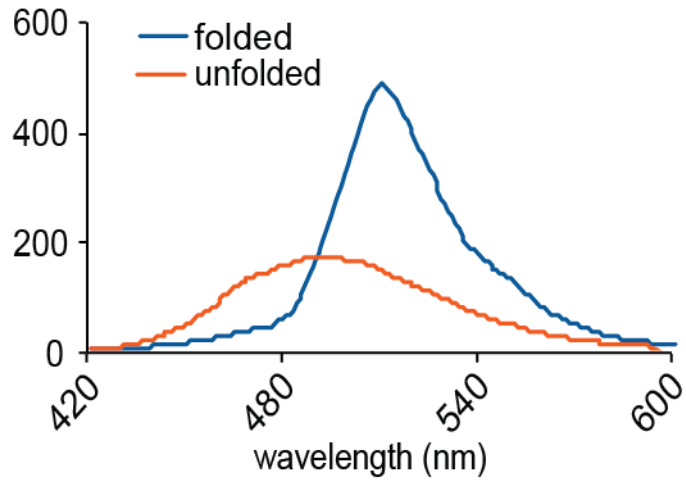


Figure 3.2 Fluorescence of EGFP-Y39Anap before and after denaturation. Before linearization there is predominantly EGFP fluorescence. After linearization there is a large increase in Anap fluorescence.

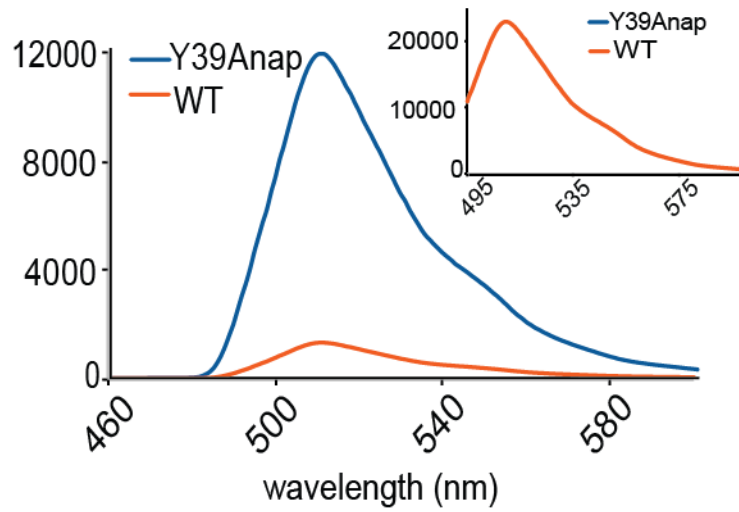


Figure 3.3 Fluorescence of EGFPwt versus EGFP-Y39Anap (normalized concentration) when excited at 365 nm. Inset: Emission spectra from the same proteins using 475 nm excitation (the blue and the red signals overlap).

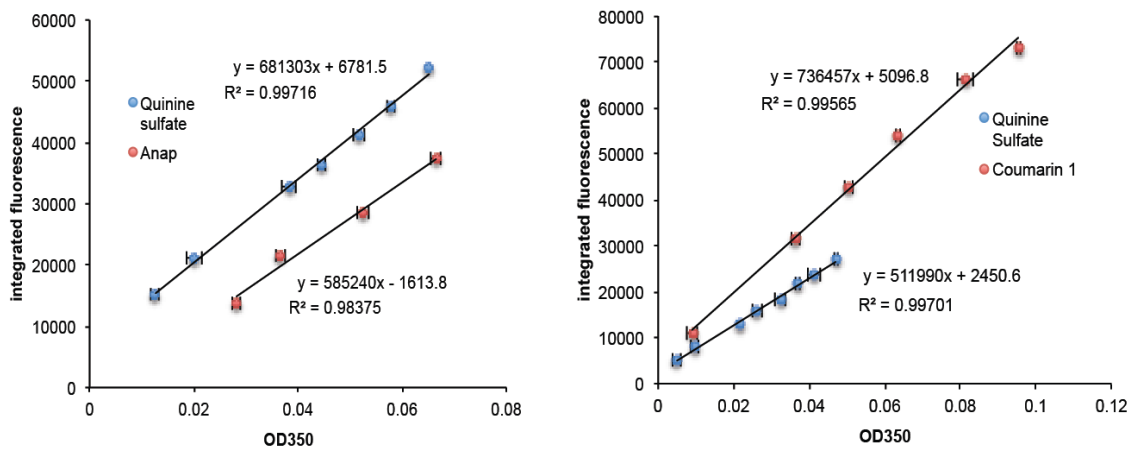


Figure 3.4 Relative quantum yield of Anap in water. Left: The quantum yield of Anap was determined from the relative slopes of the lines for Anap and quinine sulfate. Right: Quinine sulfate was cross-calibrated against coumarin-1.

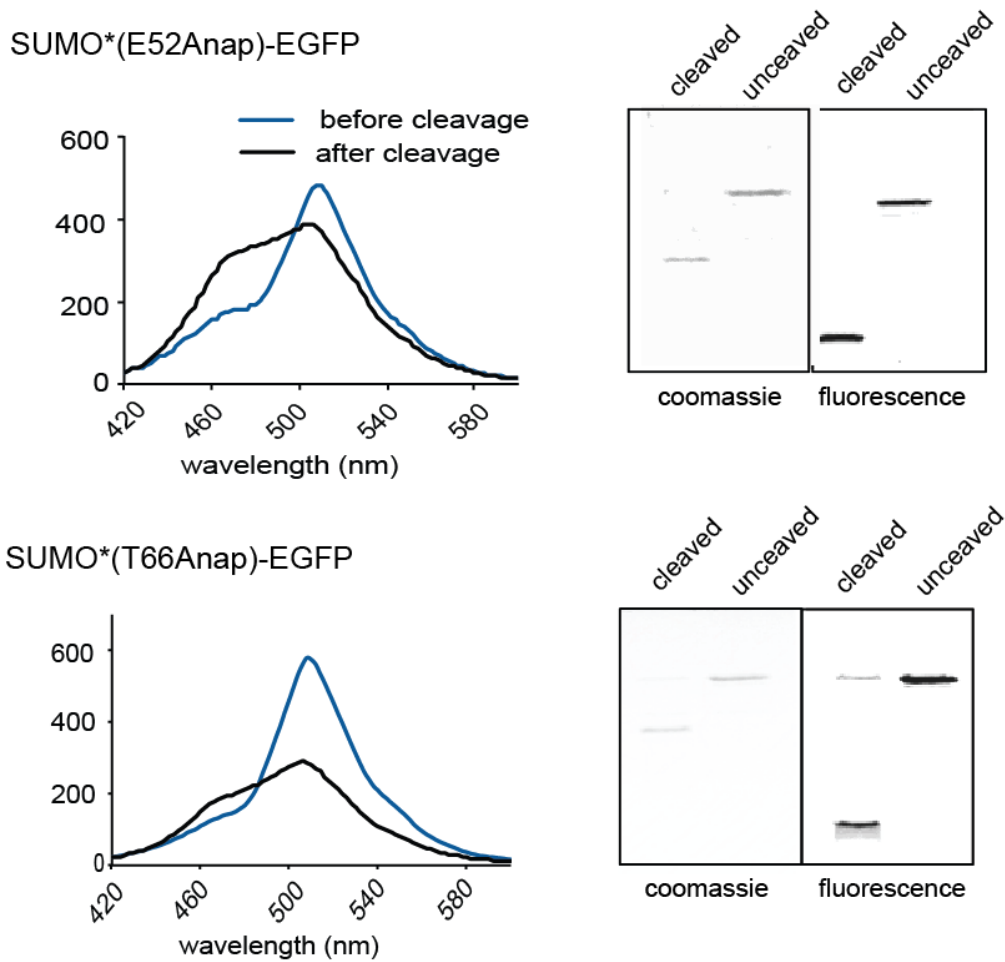


Figure 3.5 Proteolysis of SUMO* constructs containing the Anap-EGFP FRET pair. Top: SUMO*(E52Anap)-EGFP spectra (left) before cleavage and after overnight incubation with SUMO* protease. The right panel shows SDS-PAGE gel images before and after cleavage. Bottom: SUMO*(T66Anap)-EGFP corresponding data.

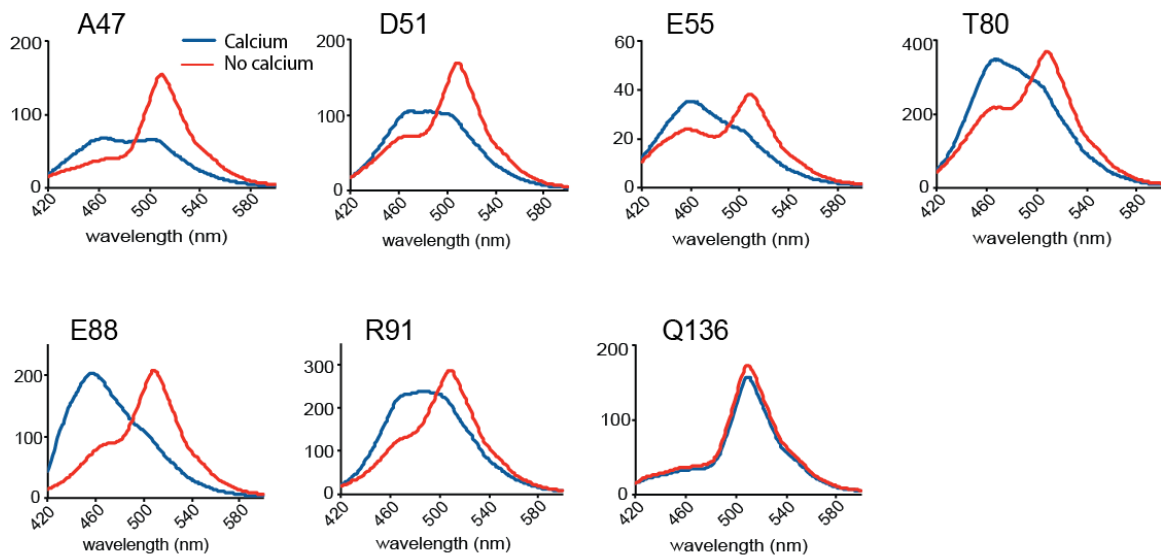


Figure 3.6 Conformational change of calmodulin constructs containing the Anap-EGFP FRET pair. The appropriate residue that was mutated to Anap is listed above each spectrum set. Emission spectra recorded in the presence or absence of 25 μM Ca^{2+} are shown in blue and red, respectively.

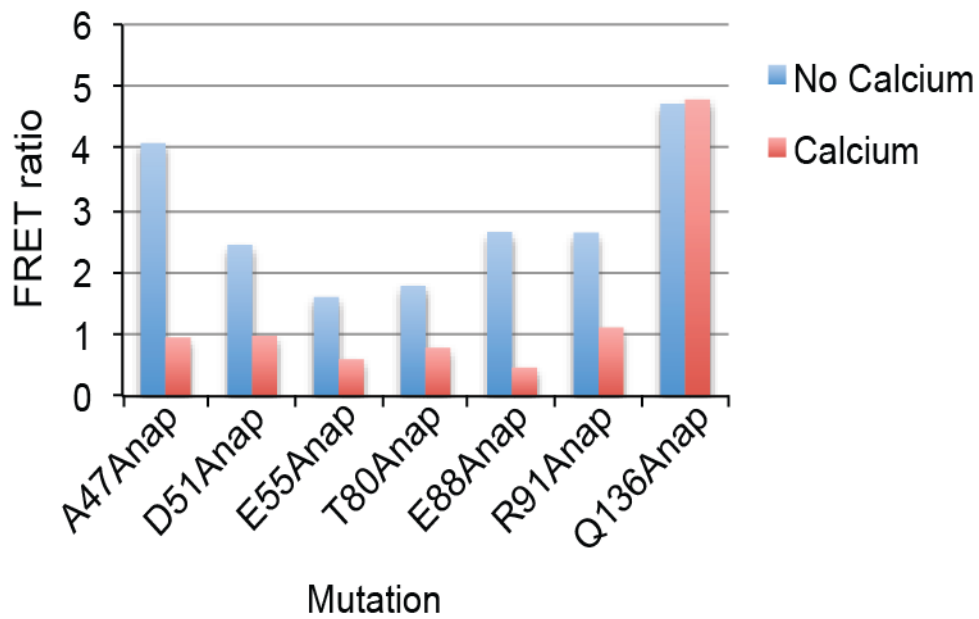


Figure 3.7 FRET ratios of calmodulin mutants with Anap-EGFP FRET pair in the presence or absence of 25 μM Ca^{2+} . In all mutants except Q136Anap the FRET ratio was larger before the addition of calcium.

Discussion

The Anap-EGFP FRET pair is similar to FP-FP FRET pairs

General quantitative measures for fluorophores include the quantum yield, extinction coefficient, and brightness of the fluorophore. Depending on the class of fluorophores, other measures may be used to rank fluorophores such as whether a FP exists in a monomeric or multimeric state. However, for FRET pairs the main quantitative measurement is the Förster radius- the distance between the two fluorophores at which the energy transfer efficiency is 50%.

The Förster radii of FRET pairs vary. For example, the FP FRET pairs EBFP-EGFP and ECFP-EYFP have Förster radii of 41 Å and 49 Å, respectively.⁹ Newer FP FRET pairs can have higher Förster radii. For example, the FP FRET pair Clover-mRuby2 has a Förster radius of 63Å.¹⁰ On the other hand, some FP FRET pairs such as EBFP-DsRed have Förster radii as low as 32 Å.⁹

The Anap-EGFP FRET pair has a Förster radius of 49 Å, which is larger than the Förster radius for the widely used color-comparable EBFP-EGFP FRET pair. This is due in part to the higher quantum yield of Anap: the quantum yield for EBFP is 0.31,¹¹ whereas the quantum yield of Anap in water is 0.50. However, the overlap integral also contributes to the Förster radius and could also contribute to the larger Förster radius value for the Anap-EGFP FRET pair.

An additional advantage of the Anap-EGFP FRET pair is that, like a FRET pair with two FPs, both fluorophores are genetically encoded. Other small molecule fluorophores such as FlAsH probes are added post-translationally, limiting their utility for real-time monitoring. This is also a challenge for inorganic fluorophores

such as QDs and LLLs, which have the added disadvantage of difficult entry into cells.^{12, 13}

The site-specificity feature of Anap adds insight to system properties

The site-specificity feature of Anap can be used to optimize the FRET system and to obtain additional information about the system properties.

One consideration for fluorophores that have flexibility where they can be incorporated into proteins is if/how the location of incorporation will affect the protein folding and/or function. This is especially true with larger fluorophores. However, we have shown that we can exploit this property with Anap. For example, The SUMO*(E52Anap)-EGFP fusion cleaved quickly and completely when incubated at room temperature with the SUMO* protease. However, upon inspection of a crystal structure of the SUMO protein, we hypothesized that T66 may be important for its interaction with SUMO protease. After generating the mutant SUMO*(T66Anap)-EGFP fusion protein, we found that cleavage was slower even in the presence of ten times the amount of SUMO* protease that was used for the E52Anap mutant. In addition, uncleaved protein still remained even after overnight incubation. This suggests that T66 is important for the 3D recognition of the SUMO* domain for proteolysis by SUMO*.

Incorporation of Anap into different loci in the Cal-M13-EGFP also provided unique insight into conformational changes system. Traditional Ca²⁺ FRET sensors (called “Cameleons”) optimized FRET pairs by pairing new FPs together.^{14, 15} Even though many Cameleons have been successfully developed this way, the limitation

that FPs can only be fused to protein termini meant that none of these systems could adjust the positioning between the two fluorophores. Given the drastic conformational change of calmodulin upon binding to M13, the ability to site-specifically incorporate the fluorophores is another tool that can be used to optimize these systems. In our studies, we found the FRET ratios in the absence of Ca^{2+} could be the same as those in the presence of Ca^{2+} (Q136Anap), or as much as five times higher (E88Anap) in the absence of Ca^{2+} . We also found differences in the fluorescence profile of Anap, which could give insight to the local environment. Given that Anap is known to have a red-shift in emission with an increase in solvent polarity, the mutants we found with slightly higher wavelength Anap maxima (D51Anap, T80Anap, R91Anap) may suggest that the Anap is in a more polar local environment. Likewise, shifts in the Anap emission maximum in the absence of Ca^{2+} versus in the presence of Ca^{2+} (E88Anap, R91Anap) suggest changes in the local environment. In less known or established systems, this could provide insight such as whether Anap is on the surface or interior of a protein in addition to the information obtained from FRET studies.

Materials and Methods

General

Cells were imaged on a Zeiss AxioObserver.A1 inverted fluorescence Microscope equipped with an X-cite series 120 illumination unit. LC/MS data were obtained on a 1260 Agilent Infinity Series HPLC/6230 Agilent TOF Mass Spectrometer. Absorbances were taken on a Nanodrop 2000c Spectrometer. FRET spectra were recorded on a Molecular Devices SpectraMax M5 plate reader. Fluorescence spectra for quantum yield data were taken on an Agilent Cary Eclipse Fluorescence Spectrophotometer

Cloning and Plasmid Construction

All chemicals and reagents were commercially obtained and used without any further purification. Primers and Gblocks for PCR reactions were purchased from IDT. PCR reactions, restriction digests, and ligations were carried out using Phusion Hot Start II polymerase (Thermo Scientific), restriction enzymes (NEB), and T4 DNA ligase (NEB).

Macherey-Nagel Nucleospin kits were used for purifying DNA (restriction digest DNA, gel purified DNA, and plasmid DNA) according to the manufacturer protocol. *E. coli* DH10B cells were used for electrotransformation and propagation of plasmid DNA.

EGFP and Cal-M13-EGFP gene sequences were PCR amplified and inserted into the pCDNA3.1-8x H1-tRNA_{CUA}^{EcLeu} vector between HindIII and XhoI sites.

SUMO*-EGFP gene sequences were PCR amplified and inserted into PacBac2R vector between SfiI sites.

Quantum Yield

The quantum yield of Anap in water was calculated relative to quinine sulfate ($\Phi = 0.55$) in 0.1 M H₂SO₄. Quinine sulfate was cross-calibrated with Coumarin-1 ($\Phi = 0.74$). The absorbance values were taken at 350nm, and emission spectra were recorded with 350nm excitation. The equation used to calculate quantum yield was:

$$\Phi_x = \Phi_{ST} (m_x / m_{ST}) (\eta_x^2 / \eta_{ST}^2)$$

Where Φ_{ST} is the quantum yield of the standard fluorophore, Φ_x is the quantum yield of the experimental fluorophore, and m_{ST} and m_x are the slopes of the lines for the standard and experimental fluorophores, respectively; η_{ST}^2 and η_x^2 are the refractive indices of the solutions which the standard and experimental fluorophores are in, respectively.

Forster Radius (R_o)

R_o for the Anap-EGFP pair was calculated using the equation:¹⁶

$$R_o = 0.211 [\Phi_{Anap} \kappa^2 \eta^{-4} J(\lambda)]^{1/6} (\text{\AA}) \quad (1)$$

Φ_{Anap} is the quantum yield of Anap, κ^2 is the orientation factor, η is the refractive index of the medium, and $J(\lambda)$ is the overlap integral between the emission spectrum of Anap and the absorbance spectrum of EGFP. For these experiments, the experimental Φ_{Anap} was used (0.50), κ^2 was assumed to be 2/3, and η was taken as that of water (1.33).

The overlap at each wavelength was calculated using the following product:¹⁷

$$F(\lambda)_{\text{Anap}}\varepsilon(\lambda)_{\text{EGFP}}\lambda^4 \quad (2)$$

Where $F(\lambda)_{\text{Anap}}$ is the normalized fluorescence value of Anap at a given wavelength, $\varepsilon(\lambda)_{\text{EGFP}}$ is the extinction coefficient value of EGFP at that wavelength, and λ^4 is the fourth power of the wavelength. The sum of the products at each wavelength was calculated and taken as the overlap integral.

Mammalian Cell Culture

HEK293 cells were cultured in DMEM media with 10% FBS and 1% Pen-Strep as supplements. Cells were maintained at 37°C with 5% CO₂. Media and supplements were obtained from Thermo Scientific.

Protein Expression and Purification

HEK293 cells were transiently transfected with PEI (Sigma) at 60-80% confluency. Transfection solutions consisted of 50 μL of 1mg/mL PEI with 12 μG of plasmid DNA and 210 μL DMEM for a 10cm² dish. Anap was added to a final concentration of 10-20 μM immediately after the transfection solution was added to the HEK293 cells. The cells were allowed to grow normally for 48 h and then harvested. The cells were then lysed in a cocktail of CellLytic-m lysis buffer (Sigma), 1x Halt protease inhibitor (Thermo Scientific), nuclease (Pierce), and 2 mM BME. Proteins were purified in their native form on either a TALON metal affinity column (Clontech) or a Ni-NTA column (Clontech) according to manufacturer protocol. EGFP and Calmodulin proteins were buffer exchanged overnight in slide-a-lyzer

3500 MWCO mini dialysis units (Thermo Scientific) at 4°C. EGFP was buffer exchanged in phosphate buffer pH 7.4; SUMO*-EGFP proteins were buffer exchanged in 20 mM Tris-HCl/150 mM NaCl pH 8.0; and Cal-M13-EGFP proteins were buffer exchanged in 10 mM MOPS/100 mM NaCl/10 mM EGTA/5 mM BME pH 7.4. For linearization study with EGFP-Y39Anap, the protein was treated with 6 M GuHCl and heated to 90°C for 10 minutes before taking spectrum.

In Vitro FRET Spectroscopy

Cleavage of the SUMO*-EGFP proteins was carried out by incubating the buffer-exchanged fusion protein with 0.2-2 U/μg of SUMO* protease 1 (Life Sensors) in 20 mM Tris-HCl/150 mM NaCl/2 mM DTT/10% glycerol at 37°C. Fluorescence spectra were recorded of the solutions with 365 nm excitation at different time intervals.

Calcium was added to the buffer-exchanged Cal-M13-EGFP proteins by reciprocal dilution of 10 mM MOPS/100 mM NaCl/10 mM EGTA/5 mM BME and 10 mM MOPS/100 mM NaCl/10 mM EGTA/5 mM BME/10 mM CaCl₂. The proteins were incubated for 5 minutes at room temperature before taking fluorescence spectra with 365 nm excitation.

References

- (1) Chatterjee, A.; Guo, J.; Lee, H. S.; Schultz, P. G. *J. Am. Chem. Soc.* **2013**, *135*, 12540-12543.
- (3) Crivat, G.; Taraska, J. W. *Trends Biotechnol.* **2012**, *30*, 8-16.
- (16) Lakowicz, J. In *Principles of Fluorescence Spectroscopy*; Springer: 2006; .
- (17) Medintz, I. L.; Hildebrandt, N., Eds.; In *FRET-Förster Resonance Energy Transfer: From Theory to Applications*; Wiley-VCH: Weinheim, Germany, 2014; .
- (4) Jones, G.; Jackson, W.; Choi, C.; Bergmark, W. *J. Phys. Chem.* **1985**, *89*, 294-300.
- (5) Melhuish, W. *J. Phys. Chem.* **1961**, *65*, 229-&.
- (6) Riedl, S.; Shi, Y. *Nat. Rev. Mol. Cell Biol.* **2004**, *5*, 897-907.
- (7) Ciechanover, A. *Nat. Rev. Mol. Cell Biol.* **2005**, *6*, 79-86.
- (8) Teague, S. *Nat. Rev. Drug Discov.* **2003**, *2*, 527-541.
- (9) Mueller, S.; Galliardt, H.; Schneider, J.; Barisas, B. G.; Seidel, T. *Front. Plant Sci.* **2013**, *4*, 413.
- (10) Lam, A. J.; St-Pierre, F.; Gong, Y.; Marshall, J. D.; Cranfill, P. J.; Baird, M. A.; McKeown, M. R.; Wiedenmann, J.; Davidson, M. W.; Schnitzer, M. J.; Tsien, R. Y.; Lin, M. Z. *Nat. Methods* **2012**, *9*, 1005-+.
- (11) Day, R. N.; Davidson, M. W. *Chem. Soc. Rev.* **2009**, *38*, 2887-2921.
- (12) Rajendran, M.; Yapici, E.; Miller, L. W. *Inorg. Chem.* **2014**, *53*, 1839-1853.
- (13) Geissler, D.; Linden, S.; Liermann, K.; Wegner, K. D.; Charbonniere, L. J.; Hildebrandt, N. *Inorg. Chem.* **2014**, *53*, 1824-1838.
- (14) McCombs, J. E.; Palmer, A. E. *Methods* **2008**, *46*, 152-159.

(15) Palmer, A. E.; Giacomello, M.; Kortemme, T.; Hires, S. A.; Lev-Ram, V.; Baker, D.; Tsien, R. Y. *Chem. Biol.* **2006**, *13*, 521-530.

Chapter 4: Optimization of the Anap FRET Partner

Abstract

The emission maximum of Anap when incorporated into proteins is between 465-480 nm. Based on this information we have previously selected EGFP as its FRET acceptor. While this was successful, we wondered if many of the other fluorescent proteins with excitation/emission maxima around the same region, and with distinct fluorescence behavior, might be a more suitable FRET partner for Anap. Such improvements may be particularly useful for *in vivo* applications of this FRET system. We therefore compared four additional FPs as FRET partners for Anap using the SUMO* mediated proteolysis of the SUMO*-FP fusion reporter as the model system. Among the four FPs tested, YPet afforded the largest change in FRET ratio upon the cleavage of the reporter. To apply this method to a more physiologically relevant proteolysis reaction, we introduced the recognition sequence of Caspase-3, DEVD, between the SUMO* domain and YPet or TagYFP. *In vitro* cleavage of these fusion proteins with caspase-3 was complete for both the TagYFP and YPet systems, and the FRET ratio changes were similar at 2.77 and 2.73, respectively. We further applied this reporter to monitor the endogenous Caspase3 activity in cell free extract.

Introduction

The emission of Anap is environment sensitive, which complicates the selection of an appropriate FRET partner.¹ While the selection of EGFP as a FRET partner for Anap was successful, we wondered if another FP would provide higher FRET efficiency. Since the emission spectrum of the donor should overlap ~30% with the absorption spectrum of the acceptor, we thought that yellow FPs may make better FRET partners than EGFP for Anap. Important criteria for choosing yellow FPs as FRET acceptors are 1-) they should exist in the monomeric state and 2-) have high extinction coefficients at their absorption maximum. Using these criteria as a baseline, we chose four different yellow FPs as FRET partners for Anap . These proteins include TagYFP (ex=508 nm, em=524 nm, $\epsilon=64,000 \text{ M}^{-1}\text{cm}^{-1}$), mCitrine (ex=516 nm, em=529 nm, $\epsilon=77,000 \text{ M}^{-1}\text{cm}^{-1}$), EYFP (ex= 514 nm, em=527 nm, $\epsilon=83,400 \text{ M}^{-1}\text{cm}^{-1}$), and YPet (ex=517 nm, em=530 nm, $\epsilon=104,000 \text{ M}^{-1}\text{cm}^{-1}$).^{2, 3} In the effort to find the best FRET partner for Anap we apply the SUMO* proteolysis experiments discussed in Chapter 3 to protein fusions containing these yellow FP FRET acceptors and quantitatively compare them. We also work towards applying this optimized FRET pair to monitor physiologically relevant activities in an *in vivo* setting where activity of caspase-3 was monitored in mammalian cell lysates after inducing apoptosis with TNF- α .⁴

Results

In vitro proteolysis of SUMO-YFP fusion proteins*

Knowledge of the behavior of different Anap-FP FRET pairs will prove valuable, especially when moving into *in vivo* applications. An important criterion in choosing a FRET partner for *in vivo* applications is minimizing SBT. We have therefore chosen to investigate the use of different YFP FRET partners for Anap. We thought our SUMO* proteolysis system would be a good system to compare different YFPs. Here, we develop four fusion proteins of SUMO* (with the E52Anap mutation) and different YFPs, and compare them before and after cleavage. This information should assist in choosing the best FP FRET partner for Anap in FRET microscopy studies.

The FRET ratios before cleavage were 1.71 for EYFP (emission intensity at 527 nm/ 480 nm), 1.62 for mCitrine (emission intensity at 529 nm/ 480nm), 1.30 for TagYFP (emission intensity at 524 nm/480 nm), and 1.94 for YPet (emission intensity at 530 nm/480 nm). After cleavage the FRET ratios were 0.83 for EYFP, 1.14 for mCitrine, 0.72 for TagYFP, and 0.73 for YPet (Figure 4.1). Consequently the change in the FRET signal as a result of the proteolysis reaction was 2.06 for EYFP, 1.42 for mCitrine, 1.81 for TagYFP, and 2.67 for YPet. Coomassie staining, as well as Anap-fluorescence imaging of SDS-PAGE analysis of these proteolysis reactions reveal near-complete cleavage for all reporters except for mCitrine.

In vitro caspase-3 cleavage of SUMO-DEVD-YFP fusion proteins*

A system where proteolysis or a conformational change can be easily induced inside living cells is important for evaluating the efficacy of our FRET systems *in vivo*. A good system for this is the extensively studied⁵ caspase-3 cleavage system, which cleaves at DEVD sites in proteins during apoptosis. Here we develop a caspase-3-recognizable system using modified SUMO*-YFPs containing a DEVD sequence in between the two domains. We confirm system functionality by cleaving with caspase-3 *in vitro*.

Before cleavage, SUMO*(E52Anap)-DEVD-YPet had a FRET ratio of 2.71 and SUMO*(E52Anap)-DEVD-TagYFP had a FRET ratio of 2.59. After 1 hr of cleavage with 0.5 U caspase-3 After 1 h of cleavage SUMO*(E52Anap)-DEVD-YPet had a FRET ratio of 0.73 and SUMO*(E52Anap)-DEVD-TagYFP had a FRET ratio of 0.69 (Figure 4.2). The calculated FRET ratio changes (FRET ratio before cleavage/ FRET ratio after 1 h cleavage) were 3.73 for SUMO*(E52Anap)-DEVD-YPet and 3.77 for SUMO*(E52Anap)-DEVD-TagYFP. Exposure of SUMO*(E52Anap)-DEVD-YPet to reaction conditions without caspase-3 showed no change in the FRET ratio over the 1 h reaction time. SDS-PAGE of the proteins suggests that the cleavage reaction went to completion for both fusion proteins within the 1 h reaction time frame.

Cell lysate Caspase-3 cleavage of SUMO-DEVD-YFP fusion proteins*

Because Anap's 365 nm maximal excitation wavelength is smaller than the lowest excitation wavelength (405 nm) on most fluorescence microscopes, clear data from living cells can only be obtained using two-photon microscopy. However,

the instrumentation required for two-photon microscopy is not widely available. We therefore used TNF- α to induce apoptosis in living cells, which in turn activates caspase-3. We show that our SUMO*(E52Anap)-DEVD-YPet FRET system acts as a reporter of caspase-3 activity in cell lysates.

The FRET ratio of the cell lysate without apoptosis induction by TNF- α was 1.9 and the FRET ratio of the cell lysate with apoptosis induction by TNF- α was 1.6 (Figure 4.3). The calculated FRET ratio change (FRET ratio before cleavage/ FRET ratio after 1 h cleavage) was 1.2. SDS-PAGE showed only two fluorescent bands of among all the proteins in the lysate. Both lysate that was treated with TNF- α and lysate that was not treated with TNF- α showed two fluorescent bands, with the lysate treated with TNF- α having a more intense small band.

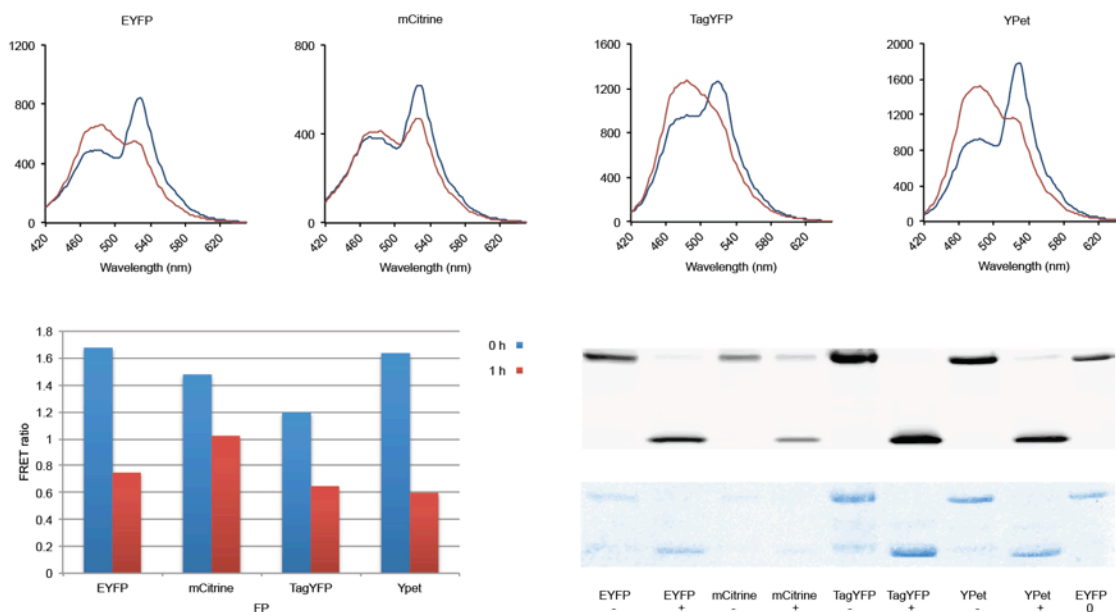


Figure 4.1 *In vitro* SUMO* cleavage of SUMO*(E52Anap)-YFP reporters. Top: FRET spectra with 365 nm excitation before (blue) and after (red) cleavage with SUMO* protease at 37°C. Bottom left: FRET ratios before (blue) and after (red) cleavage of SUMO*(E52Anap)-YFP systems. Bottom right: fluorescence (top) and coomassie (bottom) images of SDS-PAGE gel for uncleaved (-) and cleaved (+) SUMO*(E52Anap)-YFP systems. EYFP (0) is untreated SUMO*(E52Anap)-EYFP.

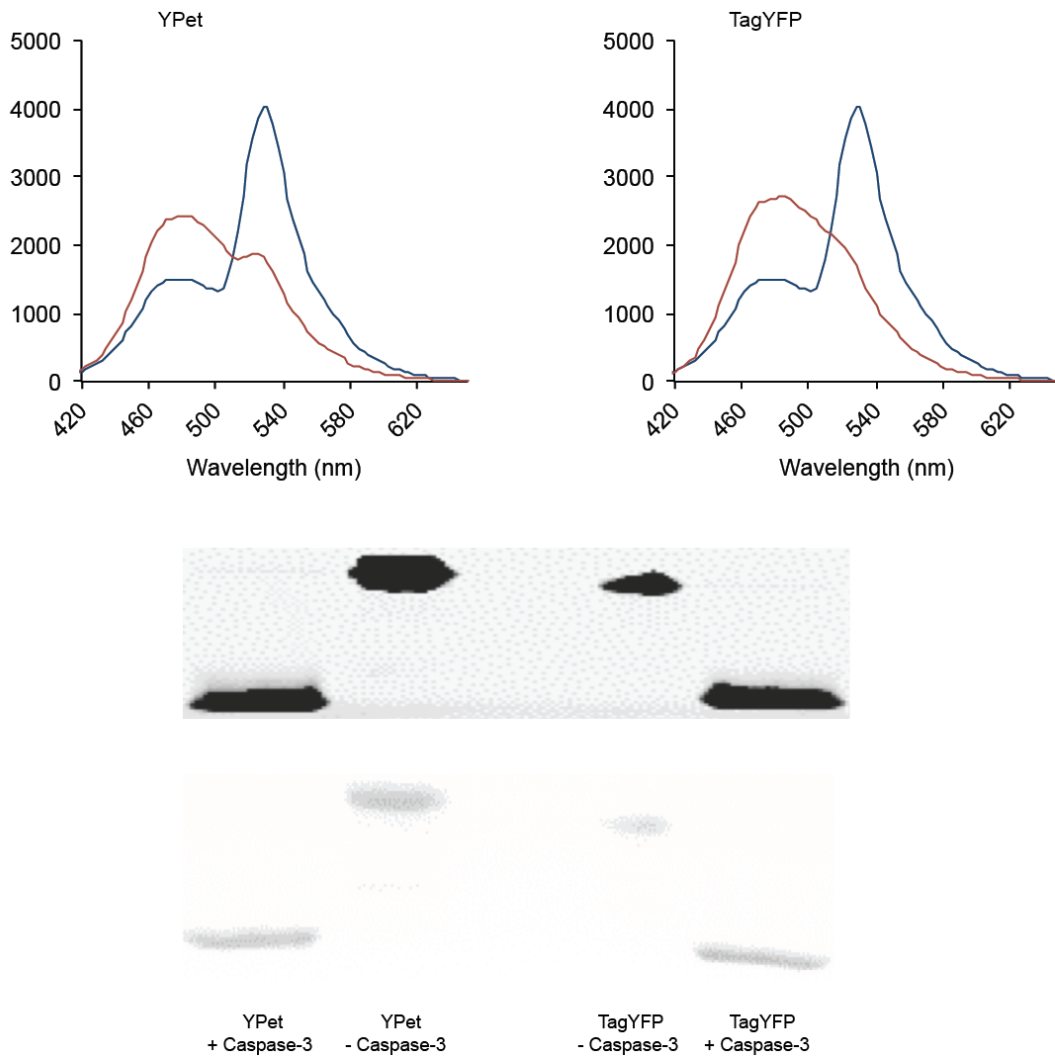
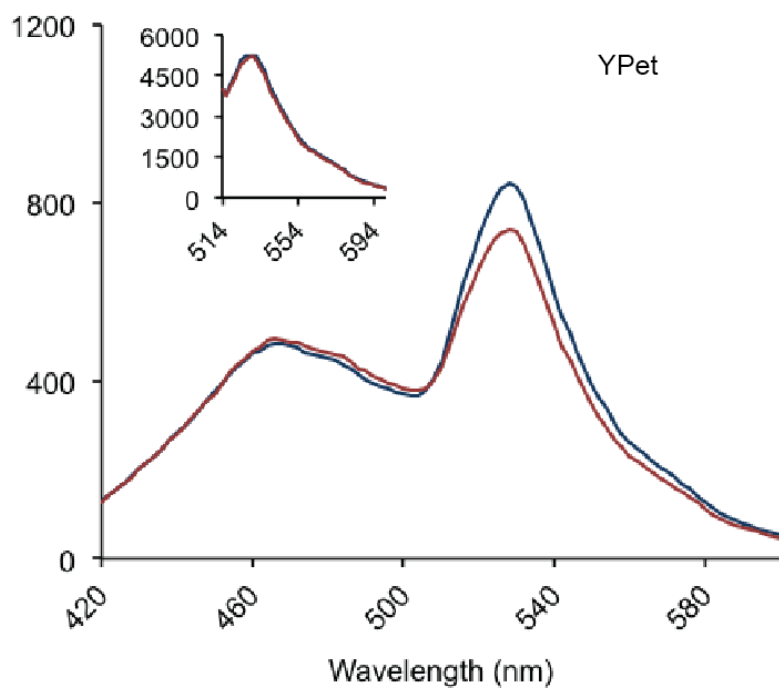


Figure 4.2 *In vitro* cleavage of SUMO*(E52Anap)-DEVD-YFP reporters with caspase-3. Top: FRET spectra of SUMO*(E52Anap)-DEVD-YPet (left) and SUMO*(E52Anap)-DEVD-TagYFP. Bottom: Fluorescence (top) and coomassie (bottom) images of SDS-PAGE gel for cleaved (+ Caspase-3) and uncleaved (-Caspase-3) SUMO*(E52Anap)-DEVD-YFP reporters.



(+) TNF- α (-) TNF- α (+) TNF- α (-) TNF- α

Figure 4.3 SUMO*(E52Anap)-DEVD-YPet cleavage in cell lysates. Top: FRET spectra before (blue) and after (red) induction of apoptosis with TNF- α . Bottom: Coomassie (left) and fluorescence (right) images of SDS-PAGE gel of apoptotic (+TNF- α) and non-apoptotic (-TNF- α) cell lysates expressing SUMO*(E52Anap)-DEVD-YPet.

Discussion

We've shown that the genetically encoded amino acid Anap can be used as a FRET donor with EGFP as a FRET acceptor, therefore producing a fully genetically encoded FRET pair similar to FP-FP FRET pairs but without the bulk of the donor fluorophore.^{3,6} However, EGFP may not be the best FRET partner for Anap; choosing the most appropriate FRET partner for Anap is challenging because the emission spectrum of Anap is environmentally sensitive. From our recent studies, we found that the emission maximum of Anap when incorporated into proteins is normally around 480 nm. The corresponding emission spectrum therefore overlaps significantly with the EGFP absorption spectrum. However, since the Stokes' shift of EGFP is small (~22 nm), its emission spectrum overlaps significantly with Anap, which poses a challenge for the *in vivo* applications of the Anap-EGFP FRET pair. Here, we show the use of four different yellow fluorescent proteins as FRET partners for Anap: EYFP, mCitrine, YPet, and TagYFP. In an effort to optimize a FRET partner for Anap we quantitatively compare the different FRET systems. Finally, in an effort to move towards *in vivo* work we carried out an apoptotic proteolysis study in cell lysates.

SUMO(E52Anap)-YPet is the most sensitive of the in vitro YFP systems tested for SUMO* protease cleavage*

The FRET ratios of SUMO*(E52Anap)-EGFP were 2.66 before cleavage and 1.21 after cleavage, resulting in a FRET ratio change of 2.20. The FRET ratio changes for the proteins in this study were 2.06 for SUMO*(E52Anap)-EYFP, 1.42 for

SUMO*(E52Anap)-mCitrine, 1.81 for SUMO*(E52Anap)-TagYFP, and 2.67 for SUMO*(E52Anap)-YPet (Figure 4.1 top, bottom left). The change in FRET is therefore similar for SUMO*(E52Anap)-YPet compared to SUMO*(E52Anap)-EGFP, but smaller for all of the other YFP variants.

The large difference in FRET ratio change of SUMO*(E52Anap)-YPet compared to the rest of the fusion proteins used in this study makes it the most suitable for *in vivo* FRET applications.

TagYFP and YPet behave similarly with SUMO(E52Anap)-DEVD-YPet cleavage by caspase-3 in vitro*

We chose two proteins to use for the DEVD cleavage studies with caspase-3 based on the information we gathered from the SUMO* cleavage studies. We chose SUMO*(E52Anap)-YPet and SUMO*(E52Anap)-TagYFP because these demonstrated high FRET ratio sensitivity. When we introduced a DEVD sequence in between the SUMO* region of the fusion and the YFP region of the fusion, the SDS-PAGE suggested that both the SUMO*(E52Anap)-DEVD-YPet and SUMO*(E52Anap)-DEVD-TagYFP cleaved completely within the 1 h time frame of the study (Figure 4.2, bottom). The FRET ratio changes were also similar for this study: 2.73 for SUMO*(E52Anap)-DEVD-YPet and 2.77 for SUMO*(E52Anap)-DEVD-TagYFP. Importantly, the control sample of SUMO*(E52Anap)-DEVD-YPet without caspase-3 maintained a FRET ratio of 2.71 throughout the duration of the study, showing that cleavage was due to the caspase-3 and not to autocleavage or the protease impurities in the sample.

The Förster radii for the Anap-YPet pair and Anap-TagYFP were calculated to be 52 Å and 49 Å, respectively. Given that the Anap-EGFP pair had a Förster radius of 49 Å, the Anap-TagYFP pair is sensitive to the same distances as the Anap-EGFP FRET pair and the Anap-YPet FRET pair is sensitive to slightly larger differences.

FRET sensitivity with the SUMO(E52Anap)-DEVD-YPet system is decreased in the cellular environment*

Even though both the SUMO*(E52Anap)-DEVD-YPet and SUMO*(E52Anap)-DEVD-TagYFP had similar FRET ratios with caspase-3 cleavage, the SUMO*(E52Anap)-DEVD-YPet had both higher expression yields and a larger Förster radius. We therefore chose to use the SUMO*(E52Anap)-DEVD-YPet for the cell lysate studies. For these studies there was a FRET ratio of 1.86 in apoptotic cells and 1.59 in non-apoptotic cells, making the FRET ratio change 1.16 (Figure 4.3, top). SDS-PAGE showed two fluorescent bands in both the lysates from the apoptotic cells and from the non-apoptotic cells, but the smaller band was more intense in the lysates from the apoptotic cells (Figure 4.3, bottom). This suggests that small amounts of caspase-3 and/or other proteases present in the cell cleaved the SUMO*(E52Anap)-DEVD-YPet fusion protein in healthy cells. In addition, the larger band corresponding to the uncleaved protein was present in the lysates from both apoptotic and non-apoptotic cells, suggesting that cleavage was incomplete. This incomplete cleavage of the fusion protein in apoptotic cells combined with undesired cleavage of the fusion protein in non-apoptotic cells account for the small difference in FRET ratio change. Nonetheless, we successfully observed increased

cleavage of SUMO*(E52Anap)-DEVD-YPet in apoptotic cells compared to non-apoptotic cells using FRET between Anap and YPet. This suggests that our Anap-YPet FRET system may prove valuable *in vivo* and in living cell applications. We particularly expect to see convincing evidence of this FRET system's utility in single cell applications where the Anap-YPet construct of interest is overexpressed, thus minimizing background. A remaining challenge is the availability of the instrumentation required to obtain quality quantifiable data.

Materials and Methods

General

Cells were imaged on a Zeiss AxioObserver.A1 inverted fluorescence Microscope equipped with an X-cite series 120 illumination unit. LC/MS data were obtained on a 1260 Agilent Infinity Series HPLC/6230 Agilent TOF Mass Spectrometer. Absorbance values were taken on a Nanodrop 2000c Spectrometer. FRET spectra were recorded on a Molecular Devices SpectraMax M5 plate reader.

Cloning and Plasmid Construction

All chemicals and reagents were commercially obtained and used without any further purification. Primers and Gblocks for PCR reactions were purchased from IDT. PCR reactions, restriction digests, and ligations were carried out using Phusion Hot Start II polymerase (Thermo Scientific), restriction enzymes (NEB), and T4 DNA ligase (NEB). Macherey-Nagel Nucleospin kits were used for purifying DNA (restriction digest DNA, gel purified DNA, and plasmid DNA) according to the manufacturer protocol. *E. coli* DH10B cells were used for electrotransformation and propagation of plasmid DNA.

Gene sequences were PCR amplified and inserted into PacBac2R vector between SfiI sites.

Förster Radius (R_o)

R_o for the Anap-EGFP pair was calculated using the equation: ⁷

$$R_o = 0.211[\Phi_{Anap}\kappa^2\eta^{-4}J(\lambda)]^{1/6} (\text{Å}) \quad (1)$$

Φ_{Anap} is the quantum yield of Anap, κ^2 is the orientation factor, η is the refractive index of the medium, and $J(\lambda)$ is the overlap integral between the emission spectrum of Anap and the absorbance spectrum of EGFP. For these experiments, the experimental Φ_{Anap} was used (0.50), κ^2 was assumed to be 2/3, and η was taken as that of water (1.33).

The overlap at each wavelength was calculated using the following product: ⁸

$$F(\lambda)_{\text{Anap}}\epsilon(\lambda)_{\text{EGFP}}\lambda^4 \quad (2)$$

Where $F(\lambda)_{\text{Anap}}$ is the normalized fluorescence value of Anap at a given wavelength, $\epsilon(\lambda)_{\text{EGFP}}$ is the extinction coefficient value of EGFP at that wavelength, and λ^4 is the fourth power of the wavelength. The sum of the products at each wavelength was calculated and taken as the overlap integral.

Mammalian Cell Culture

HEK293 cells were cultured in DMEM media with 10% FBS and 1% Pen-Strep as supplements. Cells were maintained at 37°C with 5% CO₂. Media and supplements were obtained from Thermo Scientific.

Protein Expression and Purification

HEK293 cells were transiently transfected with PEI (Sigma) at 60-80% confluency. Transfection solutions consisted of 50 μ L of 1mg/mL PEI with 12 μ G of plasmid DNA and 210 μ L DMEM for a 10cm² dish. Anap was added to a final concentration of 10-20 μ M immediately after the transfection solution was added to the HEK293 cells. The cells were allowed to grow normally for 48 h and then

harvested. The cells were then lysed in a cocktail of CellLytic-m lysis buffer (Sigma), 1x Halt protease inhibitor (Thermo Scientific), universal nuclease (Pierce), and 2 mM BME. Proteins were purified in their native form on either a TALON metal affinity column (Clontech) or a Ni-NTA column (Clontech) according to manufacturer protocol. EGFP and Calmodulin proteins were buffer exchanged overnight in slide-a-lyzer 3500 MWCO mini dialysis units (Thermo Scientific) at 4°C. EGFP was buffer exchanged in phosphate buffer pH 7.4; SUMO*-EGFP proteins were buffer exchanged in 20 mM Tris-HCl/150 mM NaCl pH 8.0; and Cal-M13-EGFP proteins were buffer exchanged in 10 mM MOPS/100 mM NaCl/10 mM EGTA/5 mM BME pH 7.4.

In Vitro FRET Spectroscopy

Cleavage of the SUMO*-FP proteins was carried out by incubating the buffer-exchanged fusion protein with 0.2-2 U/ μ g of SUMO* protease 1 (Life Sensors) in 20 mM Tris-HCl/150 mM NaCl/2 mM DTT/10% glycerol at 37°C. Fluorescence spectra were recorded of the solutions with 365 nm excitation at different time intervals.

For the *in vitro* caspase-3 studies, 0.5 nmol of protein was mixed with 0.5 U of caspase-3 (BioVision) and brought to a final volume of 82 μ L with reaction buffer. The reaction was carried out at 37°C for 1 h.

Cell Lysate Preparation and Spectroscopy

HEK293 cells were transiently transfected in the method described above with the PacBac2R plasmid containing the SUMO*(E52Anap)-DEVD-YPet and AnapRS genes. TNF- α (Fisher) was added to the cells at to a final concentration of 50 ng/ μ L 48 h after transfection and the cells were incubated at 37°C for another 6-24 h. The cells were then rinsed and harvested with phosphate buffer pH 7.4 and then lysed in a cocktail of CellLytic-m lysis buffer (Sigma), 1x Halt protease inhibitor (Thermo Scientific) and universal nuclease (Pierce) at room temperature. The lysed cells were centrifuged and fluorescence spectra of the supernatant were taken using 365 nm excitation.

References

- (1) Chatterjee, A.; Guo, J.; Lee, H. S.; Schultz, P. G. *J. Am. Chem. Soc.* **2013**, *135*, 12540-12543.
- (2) Shaner, N. C.; Steinbach, P. A.; Tsien, R. Y. *Nature Methods* **2005**, *2*, 905+.
- (3) Day, R. N.; Davidson, M. W. *Chem. Soc. Rev.* **2009**, *38*, 2887-2921.
- (4) Rath, P.; Aggarwal, B. *J. Clin. Immunol.* **1999**, *19*, 350-364.
- (5) Porter, A.; Janicke, R. *Cell Death Differ.* **1999**, *6*, 99-104.
- (6) Mueller, S.; Galliardt, H.; Schneider, J.; Barisas, B. G.; Seidel, T. *Front. Plant Sci.* **2013**, *4*, 413.
- (7) Lakowicz, J. In *Principles of Fluorescence Spectroscopy*; Springer: 2006; .
- (8) Medintz, I. L.; Hildebrandt, N., Eds.; In *FRET-Förster Resonance Energy Transfer: From Theory to Applications*; Wiley-VCH: Weinheim, Germany, 2014; .

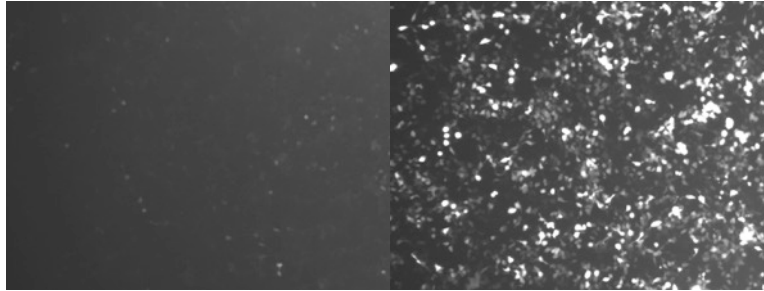
Chapter 5: Future Directions

Anap-FP FRET in vivo

The work described here does not include FRET microscopy data of any of the Anap-FP systems observed. Ideally, we would like to be able to observe these systems inside cells. The biggest challenge for this is that Anap excites maximally at 360-365 nm, but the shortest wavelength laser in most confocal microscopes is 405 nm. A better option would be to use a microscope with two-photon excitation capabilities so that Anap can be maximally excited, therefore maximizing the signal.

Dansylalanine as an alternative fluorophore to Anap

Our goal is to incorporate different UAAs with different spectral properties into mammalian cells as FRET partners so that different pairs can be made as appropriate for different applications. A good option for the next fluorophore is dansylalanine. Dansylalanine has already been incorporated genetically into *Saccharomyces Cerevisiae*. When dansylalanine was incorporated into the hSOD protein inside *S. cerevisiae* it had emission maxima ranging from 528-544 nm, about 48-84 nm more red shifted compared to the range of emission maxima observed with Anap in proteins.¹ In addition, the low excitation wavelength of 340 nm for dansylalanine means that this fluorophore has a large Stokes' shift, which would be good for avoiding spectral bleedthrough in *in vivo* studies.



0µM Dan

40µM Dan

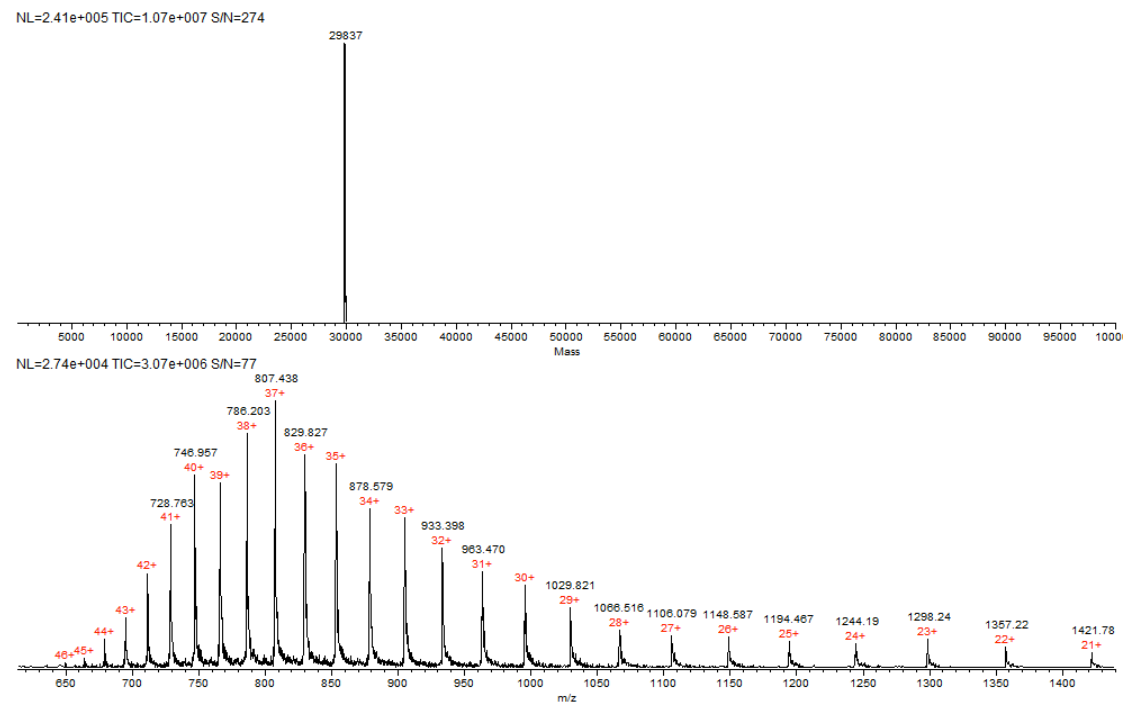


Figure 5.1 Incorporation of dansylalanine (Dan) into EGFP-TAG39 protein HEK293 cells. Top: Fluorescent images of HEK293 cells transfected with EGFP-TAG39 and DanRS in the absence of Dan (left) and in the presence of Dan (right). Bottom: Mass spectrum of purified EGFP-Y39Dan. Methods used for transfection and Ni-NTA purification are discussed in chapters three and four.

We were able to use the previously evolved tRNA/DanRS to incorporate dansylalanine into EGFP-TAG39 of mammalian cells. Future studies will focus on imaging dansylalanine *in vivo* and ultimately be used to study FRET *in vivo* with a dansylalanine donor and orange or red acceptor such as mOrange, mRuby, or mStrawberry.

Other alternative fluorophores to Anap

The biggest challenge of dansylalanine is the same as that of Anap: the excitation is lower than what most confocal microscopes have to maximally excite the fluorophore. Besides using two-photon excitation, a more long-term solution would be to develop new fluorophores with lower energy excitation maxima. Of course, this would also require the evolution of new tRNA/UaaRS pairs for genetic incorporation into cells. Because size is a restriction in these systems, a major challenge is to develop red-shifted fluorophores that are small, water soluble, and stable.

Fully genetically encoded two-UAA FRET

Because all of the systems mentioned here involve one UAA and one FP, the limitations due to the large size of FPs is only partially ameliorated. A two-UAA FRET system in which both UAAs can be incorporated genetically using tRNA/UaaRS pairs that do not cross-react would be ideal for solving the challenges associated with the large size of FPs as well as the challenges associated with FPs being limited to protein termini. While FRET systems utilizing two UAAs have been

successfully developed, to our knowledge no system has been developed where both fluorophores have been incorporated genetically in their mature form.^{2,3}

References

- (1) Summerer, D.; Chen, S.; Wu, N.; Deiters, A.; Chin, J. W.; Schultz, P. G. *Proc. Natl. Acad. Sci. U. S. A.* **2006**, *103*, 9785-9789.
- (2) Wang, K.; Sachdeva, A.; Cox, D. J.; Wilf, N. M.; Lang, K.; Wallace, S.; Mehl, R. A.; Chin, J. W. *Nat. Chem.* **2015**, *7*, 178-178.
- (3) Wissner, R. F.; Batjargal, S.; Fadzen, C. M.; Petersson, E. J. *J. Am. Chem. Soc.* **2013**, *135*, 6529-6540.

Supporting Information

Gene sequences

EGFP-TAG39

ATGGTGAGCAAGGGCGAGGAGCTGTTACCGGGGTGGTGCCCATCCTGGTTCGAGCTGGAC
GGCGACGTAAACGGCCACAAGTTCAGCGTGTCCGGCGAGGGCGAGGGCGATGCCACCTAG
GGCAAGCTGACCTGAAGTTCATCTGCACCACCGGCAAGCTGCCCGTGCCCTGGCCCACCC
TCGTGACCACCCTGACCTACGGCGTGCAGTGCTTCAGCCGCTACCCCGACCACATGAAGC
AGCACGACTTCTTCAAGTCCGCCATGCCCGAAGGCTACGTCCAGGAGCGCACCATCTTCT
TCAAGGACGACGGCAACTACAAGACCCGCGCCGAGGTGAAGTTCGAGGGCGACACCCTGG
TGAACCGCATCGAGCTGAAGGGCATCGACTTCAAGGAGGACGGCAACATCCTGGGGCACA
AGCTGGAGTACAACAGCCACAACGTCTATATCATGGCCGACAAGCAGAAGAAC
GGCATCAAGGTGAACTTCAAGATCCGCCACAACATCGAGGACGGCAGCGTGCAGCTCGCC
GACCACTACCAGCAGAACACCCCATCGGGCAGGGCCCCGTGCTGCTGCCCGACAACCACT
ACCTGAGCACCCAGTCCGCCCTGAGCAAAGACCCCAACGAGAAGCGCGATCACATGGTCC
TGCTGGAGTTCGTGACCGCCCGGGATCACTCTCGGCATGGACGAGCTGTACAAGGGGC
CCTTCGAACAAAAACTCATCTCAGAAGAGGATCTGAATATGCATACCGGTCATCATCACC
ATCACCATTGA

Key:

.....6x His Tag

SUMO*-EGFP

ATGTCCCTGCAGGACTCAGAAGTCAATCAAGAAGCTAAGCAAGAGGTCAAGCCAGAAGT
CAAGCCTGAGACTCACATCAATTTAAAGGTGTCCGATGGATCTTCAGAGATCTTCTTCAA
GATCAAAAAGACCACTCCTTTAAGAAGGCTGATGGAAGCGTTCGCTAAAAGACAGGGTA
AGGAAATGGACTCCTTAACCTTCTTGTACGACGGTATTGAAATTCAAGCTGATCAGACCC
CTGAAGATTTGGACATGGAGGATAACGATATTATTGAGGCTCACAGAGAACAGATTGGA
GGTGTGAGCAAGGGCGAGGAGCTGTTACCGGGGTGGTGCCCATCCTGGTTCGAGCTGGAC
GGCGACGTAAACGGCCACAAGTTCAGCGTGTCCGGCGAGGGCGAGGGCGATGCCACCTAC
GGCAAGCTGACCTGAAGTTCATCTGCACCACCGGCAAGCTGCCCGTGCCCTGGCCCACCC
TCGTGACCACCCTGACCTACGGCGTGCAGTGCTTCAGCCGCTACCCCGACCACATGAAGC
AGCACGACTTCTTCAAGTCCGCCATGCCCGAAGGCTACGTCCAGGAGCGCACCATCTTCT
TCAAGGACGACGGCAACTACAAGACCCGCGCCGAGGTGAAGTTCGAGGGCGACACCCTGG
TGAACCGCATCGAGCTGAAGGGCATCGACTTCAAGGAGGACGGCAACATCCTGGGGCACA
AGCTGGAGTACAACAGCCACAACGTCTATATCATGGCCGACAAGCAGAAGAAC
GGCATCAAGGTGAACTTCAAGATCCGCCACAACATCGAGGACGGCAGCGTGCAGCTCGCC
GACCACTACCAGCAGAACACCCCATCGGGCAGGGCCCCGTGCTGCTGCCCGACAACCACT
ACCTGAGCACCCAGTCCGCCCTGAGCAAAGACCCCAACGAGAAGCGCGATCACATGGTCC
TGCTGGAGTTCGTGACCGCCCGGGATCACTCTCGGCATGGACGAGCTGTACAAGGGGC
CCTTCGAACAAAAACTCATCTCAGAAGAGGATCTGAATATGCATACCGGTCATCATCACC
ATCACCATCATCATCACCATCACCATTGA

Key:

_____SUMO*

.....EGFP

.....12x His Tag

Mutations used in this Study:

Codon Mutation	Amino Acid Mutation
GAA → TAG	E52Anap
ACC → TAG	T66Anap

Cal-M13-EGFP

ATGGATGACCAACTGACAGAAGAGCAGATTGCAGAGTTCAAAGAAGCCTTCTCATTATT
CGACAAGGATGGGGACGGCACCATCACCACAAAGGAACCTTGGCACCGTTATGAGGTCGCT
TGGACAAAACCCAACGGAA**GCA**GAATTGCAG**GAT**ATGATCAAT**GAA**GTCGATGCTGATG
GCAATGGAACGATTTACTTTTCTGAATTTCTTACTATGATGGCTAGAAAAATGAAGGAC
ACAGACAGCGAAGAGGAAATCCGA**GA**GCATT**CCG**TGTTTTGACAAGGATGGGAACGG
CTACATCAGCGCTGCTGAATTACGTCACGTCATGACAAACCTCGGGGAGAAGTAAACAGA
TGAAGAAGTTGATGAAATGATAAGGGAAGCAGATATCGATGGTGATGGC**CAA**GTA
AACTATGAAGAGTTTGTACAAATGATGACAGCAAAGGGGGGAAGAGGCGCTGGAAGAAAAAC
TTCATTGCCGTCAGCGCTGCCAACCGGTTCAAGAAGATCTCCAGCTCCGGGGCACTGTCT
AGAATGCTGAGCAAGGGCGAGGAGCTGTTACCGGGTGGTGCCCATCCTGGTTCGAGCTG
GACGGCGACGTAAACGGCCACAAGTTCAGCGTGTCGGCGAGGGCGAGGGCGATGCCACC
TACGGCAAGCTGACCCTGAAGTTCATCTGCACCACCGGCAAGCTGCCCGTGCCCTGGCCC
ACCCTCGTGACCACCCTGACCTACGGCGTGCACTGCTTCAGCCGCTACCCGACCACATGA
AGCAGCAGCACTTCTTCAAGTCCGCCATGCCCCAAGGCTACGTCCAGGAGCGCACCATCT
TCTTCAAGGACGACGGCAACTACAAGACCCGCGCCGAGGTGAAGTTCGAGGGCGACACCC
TGGTGAACCGCATCGAGCTGAAGGGCATCGACTTCAAGGAGGACGGCAACATCCTGGGGC
ACAAGCTGGAGTACAACACTACAACAGCCACAACGTCTATATCATGGCCGACAAGCAGAAG
AACGGCATCAAGGTGAACCTCAAGATCCGCCACAACATCGAGGACGGCAGCGTGCAGCTC
GCCGACCACTACCAGCAGAACACCCCATCGGCGACGGCCCCGTGCTGCTGCCCGACAACC
ACTACCTGAGCACCCAGTCCGCCCTGAGCAAAGACCCCAACGAGAAGCGCGATCACATGG
TCCTGCTGGAGTTCGTGACCGCCCGGGATCACTCTCGGCATGGACGAGCTGTACAAGC
ATCATCACCATCACCATTAA

Key:

_____ Calmodulin
===== M13
..... EGFP
~~~~~ 6x His Tag

Mutations used in this study:

| Codon Mutation   | Amino Acid Mutation |
|------------------|---------------------|
| <b>GCA</b> → TAG | A47Anap             |
| <b>GAT</b> → TAG | D51Anap             |
| <b>GAA</b> → TAG | E55Anap             |

ACA→TAG  
GAA→TAG  
CGT→TAG  
CAA→TAG

T80Anap  
E88Anap  
R91Anap  
Q136Anap

### SUMO\*-EYFP

ATGTCCCTGCAGGACTCAGAAGTCAATCAAGAAGCTAAGCAAGAGGTCAAGCCAGAAGT  
CAAGCCTGAGACTCACATCAATTTAAAGGTGTCCGATGGATCTTCAGAGATCTTCTTCAA  
GATCAAAAAGACCACTCCTTTAAGAAGGCTGATG**GAA**GCGTTCGCTAAAAGACAGGGTA  
AGGAAATGGACTCCTTAACGTTCTTGTACGACGGTATTGAAATTC AAGCTGATCAGACCC  
CTGAAGATTTGGACATGGAGGATAACGATATTATTGAGGCTCACAGAGAACAGATTGGA  
GGTATGGTGAGCAAGGGCGAGGAGCTGTTACCGGGTGGTGGCCATCCTGGTTCGAGCTG  
GACGGCGACGTAAACGGCCACAAGTTCAGCGTGTCCGGCGAGGGCGAGGGCGATGCCACC  
TACGGCAAGCTGACCCTGAAGTTCATCTGCACCACCGGCAAGCTGCCCGTGCCTGGCCC  
ACCCTCGTGACCACCTTCGGCTACGGCGTGCAGTGCTTCGCCCGCTACCCCGACCACATGA  
AGCAGCACGACTTCTTCAAGTCCGCCATGCCCCAAGGCTACGTCCAGGAGCGCACCATCT  
TCTTCAAGGACGACGGCAACTACAAGACCCGCGCCGAGGTGAAGTTCGAGGGCGACACCC  
TGGTGAACCGCATCGAGCTGAAGGGCATCGACTTCAAGGAGGACGGCAACATCCTGGGGC  
ACAAGCTGGAGTACAACACTACAACAGCCACAACGTCTATATCATGGCCGACAAGCAGAAG  
AACGGCATCAAGGTGAACCTTCAAGATCCGCCACAACATCGAGGACGGCAGCGTGCAGCTC  
GCCGACCACTACCAGCAGAACACCCCATCGGCGACGGCCCCGTGCTGCTGCCCGACAACC  
ACTACCTGAGCTACCAGTCCGCCCTGAGCAAAGACCCCAACGAGAAGCGCGATCACATGG  
TCCTGCTGGAGTTCGTGACCGCCCGGGATCACTCTCGGCATGGACGAGCTGTACAAGg  
gttctCATCATCACCATCACCATCATCACCATCACCATCATtaa

Key:

\_\_\_\_\_ SUMO\*  
..... EYFP  
..... 12x His Tag

Mutations used in this Study:

Codon Mutation      Amino Acid Mutation  
**GAA**→TAG              E52Anap

### SUMO\*-mCitrine

ATGTCCCTGCAGGACTCAGAAGTCAATCAAGAAGCTAAGCAAGAGGTCAAGCCAGAAGT  
CAAGCCTGAGACTCACATCAATTTAAAGGTGTCCGATGGATCTTCAGAGATCTTCTTCAA  
GATCAAAAAGACCACTCCTTTAAGAAGGCTGATG**GAA**GCGTTCGCTAAAAGACAGGGTA  
AGGAAATGGACTCCTTAACGTTCTTGTACGACGGTATTGAAATTC AAGCTGATCAGACCC  
CTGAAGATTTGGACATGGAGGATAACGATATTATTGAGGCTCACAGAGAACAGATTGGA  
GGTATGGTGAGCAAGGGCGAGGAGCTGTTACCGGGTGGTGGCCATCCTGGTTCGAGCTG  
GACGGCGACGTAAACGGCCACAAGTTCAGCGTGTCCGGCGAGGGCGAGGGCGATGCCACC  
TACGGCAAGCTGACCCTGAAGTTCATCTGCACCACCGGCAAGCTGCCCGTGCCTGGCCC  
ACCCTCGTGACCACCTTCGGCTACGGCGTGCAGTGCTTCGCCCGCTACCCCGACCACATGA  
AGCAGCACGACTTCTTCAAGTCCGCCATGCCCCAAGGCTACGTCCAGGAGCGCACCATCT  
TCTTCAAGGACGACGGCAACTACAAGACCCGCGCCGAGGTGAAGTTCGAGGGCGACACCC

TGGTGAACCGCATCGAGCTGAAGGGCATCGACTTCAAGGAGGACGGCAACATCCTGGGGC  
ACAAGCTGGAGTACAACACTACAACAGCCACAACGTCTATATCATGGCCGACAAGCAGAAG  
AACGGCATCAAGGTGAACCTTCAAGATCCGCCACAACATCGAGGACGGCAGCGTGCAGCTC  
GCCGACCACTACCAGCAGAACACCCCATCGGCGACGGCCCCGTGCTGCTGCCCGACAACC  
ACTACCTGAGCTACCAGTCCAAGCTGAGCAAAGACCCCAACGAGAAGCGCGATCACATGG  
TCCTGCTGGAGTTCGTGACCGCCGCGGGATCACTCTCGGCATGGACGAGCTGTACAAGg  
gttctCATCATCACCATCACCATCATCACCATCACCATCATtaa

Key:

\_\_\_\_\_ SUMO\*  
..... mCitrine  
..... 12x His Tag

Mutations used in this Study:

Codon Mutation      Amino Acid Mutation  
**GAA**→TAG              E52Anap

### SUMO\*-TAGYFP

ATGTCCCTGCAGGACTCAGAAGTCAATCAAGAAGCTAAGCAAGAGGTCAAGCCAGAAGT  
CAAGCCTGAGACTCACATCAATTTAAAGGTGTCCGATGGATCTTCAGAGATCTTCTTCAA  
GATCAAAAAGACCACTCCTTTAAGAAGGCTGATG**GAA**GCGTTCGCTAAAAGACAGGGTA  
AGGAAATGGACTCCTTAACGTTCTTGTACGACGGTATTGAAATTCAGCTGATCAGACCC  
CTGAAGATTTGGACATGGAGGATAACGATATTATTGAGGCTCACAGAGAACAGATTGGA  
GGTATGGTTAGCAAAGGCGAGGAGCTGTTCCGCCGCATCGTGCCCGTGCTGATCGAGCTG  
GACGGCGACGTGCACGGCCACAAGTTCAGCGTGCGCGGCGAGGGCGAGGGCGACGCCGAC  
TACGGCAAGCTGGAGATCAAGTTCATCTGCACCACCGGCAAGCTGCCCGTGCCCTGGCCC  
ACCCTGGTGACCACCCTCACCTACGGCGTACAGTGCTTCGCCCGCTACCCCAAGCACATGA  
AGATGAACGACTTCTTCAAGAGCGCCATGCCCGAGGGCTACATCCAGGAGCGCACCATCC  
TCTTCCAAGACGACGGCAAGTACAAGACCCGCGGCGAGGTGAAGTTCGAGGGCGACACCC  
TGGTGAACCGCATCGAGCTGAAGGGCAAGGACTTCAAGGAGGACGGCAACATCCTGGGGC  
ACAAGCTGGAGTACAGCTTCAACAGCCACAACGTCTACATCACCCCGACAAGGCCAACA  
ACGGCCTGGAGGTGAACCTTCAAGACCCGCCACAACATCGAGGGCGGCGGCGTGCAGCTGG  
CCGACCACTACCAGACCAACGTGCCCTGGGCGACGGCCCCGTGCTGATCCCCATCAACCA  
CTACCTGAGCTACCAGACCGACATCAGCAAGGACCGCAACGAGGCCCGCGACCACATGGT  
GCTCCTGGAGTCCGTGAGCGCCTGCAGCCACACCCACGGCATGGACGAGCTGTACCGCggtt  
ctCATCATCACCATCACCATCATCACCATCACCATCATtaa

Key:

\_\_\_\_\_ SUMO\*  
..... TAGYFP  
..... 12x His Tag

Mutations used in this Study:

Codon Mutation      Amino Acid Mutation  
**GAA**→TAG              E52Anap

### SUMO\*-YPet

ATGTCCCTGCAGGACTCAGAAGTCAATCAAGAAGCTAAGCAAGAGGTCAAGCCAGAAGT  
CAAGCCTGAGACTCACATCAATTTAAAGGTGTCCGATGGATCTTCAGAGATCTTCTTCAA  
GATCAAAAAGACCACTCCTTTAAGAAGGCTGATG**GAA**GCGTTCGCTAAAAGACAGGGTA  
AGGAAATGGACTCCTTAACGTTCTTGTACGACGGTATTGAAATTCAGCTGATCAGACCC  
CTGAAGATTTGGACATGGAGGATAACGATATTATTGAGGCTCACAGAGAACAGATTGGA  
GGTATGGTGAGCAAAGGCCAAGAGCTGTTACCGGCGTGGTGCCCATCCTGGTGGAGCTG  
GACGGCGACGTGAACGGCCACAAGTTCAGCGTGAGCGGCGAGGGCGAGGGCGACGCCACC  
TACGGCAAGCTGACCCTGAAGCTGCTGTGCACCACCGGCAAGCTGCCCGTGCCCTGGCCC  
ACCCTGGTGACCACCCTGGGCTACGGCGTGCACTGCTTCGCCCGGTACCCCGACCACATG  
AAGCAGCAGACTTCTTCAAGAGCGCCATGCCCGAGGGCTACGTGCAGGAGCGGACCATC  
TTCTTCAAGGACGACGGCAACTACAAGACCCGGGCCGAGGTGAAGTTCGAGGGCGACACC  
CTGGTGAACCGGATCGAGCTGAAGGGCATCGACTTCAAGGAGGACGGCAACATCCTGGGC  
CACAAGCTGGAGTACAACACTACAACAGCCACAACGTGTACATCACCGCCGACAAGCAGAAG  
AACGGCATCAAGGCCAACTTCAAGATCCGGCACAACATCGAGGACGGCGGCGTGCAGCTG  
GCCGACCACTACCAGCAGAACACCCCATCGGCGACGGCCCCGTGCTGCTGCCCGACAACC  
ACTACCTGAGCTACCAGAGCGCCCTGTTCAAGGACCCCAACGAGAAGCGGGACCACATGG  
TGCTGCTGGAGTTCCTGACCGCCCGGCATCACCGAGGGCATGAACGAGCTCTATAAGg  
gttctCATCATCACCATCACCATCATCACCATCACCATCATtaa

Key:

\_\_\_\_\_ SUMO\*

..... YPet

..... 12x His Tag

Mutations used in this Study:

Codon Mutation      Amino Acid Mutation

**GAA** → TAG

E52Anap

### SUMO\*(E52Anap)-DEV-YPet

atgTCCCTGCAGGACTCAGAAGTCAATCAAGAAGCTAAGCCAGAGGTCAAGCCAGAAGTC  
AAGCCTGAGACTCACATCAATTTAAAGGTGTCCGATGGATCTTCAGAGATCTTCTTCAAG  
ATCAAAAAGACCACTCCTTTAAGAAGGCTGATG**GAA**GCGTTCGCTAAAAGACAGGGTAA  
GGAAATGGACTCCTTAACGTTCTTGTACGACGGTATTGAAATTCAGCTGATCAGACCCC  
TGAAGATTTGGACATGGAGGATAACGATATTATTGAGGCTCACAGAGAACAGATTGGAG  
GTgatgaggtc gatggcgcATGGTGAGCAAAGGCCAAGAGCTGTTACCGGCGTGGTGCCCAT  
CCTGGTGGAGCTGGACGGCGACGTGAACGGCCACAAGTTCAGCGTGAGCGGCGAGGGCGA  
GGGCGACGCCACCTACGGCAAGCTGACCCTGAAGCTGCTGTGCACCACCGGCAAGCTGCC  
CGTGCCCTGGCCACCCTGGTGACCACCCTGGGCTACGGCGTGCACTGCTTCGCCCGGTAC  
CCCGACCACATGAAGCAGCAGACTTCTTCAAGAGCGCCATGCCCGAGGGCTACGTGCAG  
GAGCGGACCATCTTCTTCAAGGACGACGGCAACTACAAGACCCGGGCCGAGGTGAAGTTC  
GAGGGCGACACCCTGGTGAACCGGATCGAGCTGAAGGGCATCGACTTCAAGGAGGACGGC  
AACATCCTGGGCCACAAGCTGGAGTACAACACTACAACAGCCACAACGTGTACATCACCGCC  
GACAAGCAGAAGAACGGCATCAAGGCCAACTTCAAGATCCGGCACAACATCGAGGACGG  
CGGCGTGCAGCTGGCCGACCACTACCAGCAGAACACCCCATCGGCGACGGCCCCGTGCT

GCTGCCCGACAACCACTACCTGAGCTACCAGAGCGCCCTGTTCAAGGACCCCAACGAGAA  
GCGGGACCACATGGTGGCTGCTGGAGTTCCTGACCGCCGCGGCATCACCGAGGGCATGAA  
CGAGCTCTATAAGggttctCATCATCACCATCACCATCATCACCATCACCATCATtaa

Key:

\_\_\_\_\_ SUMO\*  
..... DEVD  
..... Ypet  
..... 12x His Tag

Mutations used in this Study:

Codon Mutation      Amino Acid Mutation  
**GAA**→TAG              E52Anap

**SUMO\*(E52Anap)-DEVD-TAGYFP**

atgTCCCTGCAGGACTCAGAAGTCAATCAAGAAGCTAAGCCAGAGGTCAAGCCAGAAGTC  
AAGCCTGAGACTCACATCAATTTAAAGGTGTCCGATGGATCTTCAGAGATCTTCTTCAAG  
ATCAAAAAGACCACTCCTTTAAGAAGGCTGATG**GAA**GCGTTCGCTAAAAGACAGGGTAA  
GGAAATGGACTCCTTAACGTTCTTGTACGACGGTATTGAAATTCAAGCTGATCAGACCCC  
TGAAGATTTGGACATGGAGGATAACGATATTATTGAGGCTCACAGAGAACAGATTGGAG  
GTgatgaggtc gatggcggcATGGTTAGCAAAGGCGAGGAGCTGTTTCGCCGGCATCGTGCCCGT  
GCTGATCGAGCTGGACGCGACGTGCACGGCCACAAGTTCAGCGTGCGCGGCGAGGGCGA  
GGGCGACGCCACTACGGCAAGCTGGAGATCAAGTTCATCTGCACCACGGCAAGCTGCC  
CGTGCCCTGGCCCACCCTGGTGACCACCCTCACCTACGGCGTACAGTGCTTCGCCCCGCTAC  
CCCAAGCACATGAAGATGAACGACTTCTTCAAGAGCGCCATGCCCGAGGGCTACATCCAG  
GAGCGACCATCCTCTTCCAAGACGACGGCAAGTACAAGACCCGCGGCGAGGTGAAGTTC  
GAGGGCGACACCCTGGTGAACCGCATCGAGCTGAAGGGCAAGGACTTCAAGGAGGACGG  
CAACATCCTGGGCCACAAGCTGGAGTACAGCTTCAACAGCCACAACGTCTACATCACCCC  
CGACAAGGCCAACAACGGCCTGGAGGTGAAGTTCAGACCCGCCACAACATCGAGGGCGG  
CGGCGTGCAGCTGGCCGACCACTACCAGACCAACGTGCCCTGGGGCGACGGCCCCGTGCT  
GATCCCCATCAACCACTACCTGAGCTACCAGACCGACATCAGCAAGGACCGCAACGAGGC  
CCGCGACCACATGGTGGCTCCTGGAGTCCGTCAGCGCCTGCAGCCACACCCACGGCATGGA  
CGAGCTGTACCGCggttctCATCATCACCATCACCATCATCACCATCACCATCATtaa

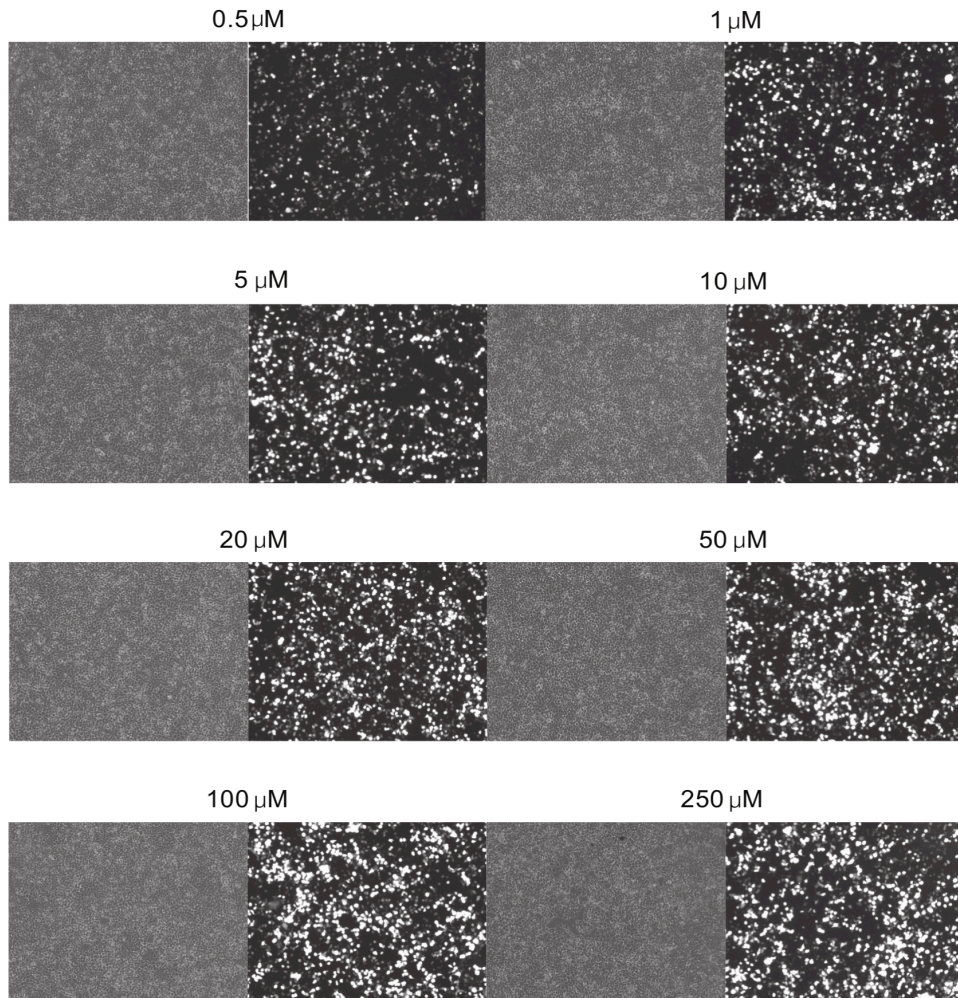
Key:

\_\_\_\_\_ SUMO\*  
..... DEVD  
..... TagYFP  
..... 12x His Tag

Mutations used in this Study:

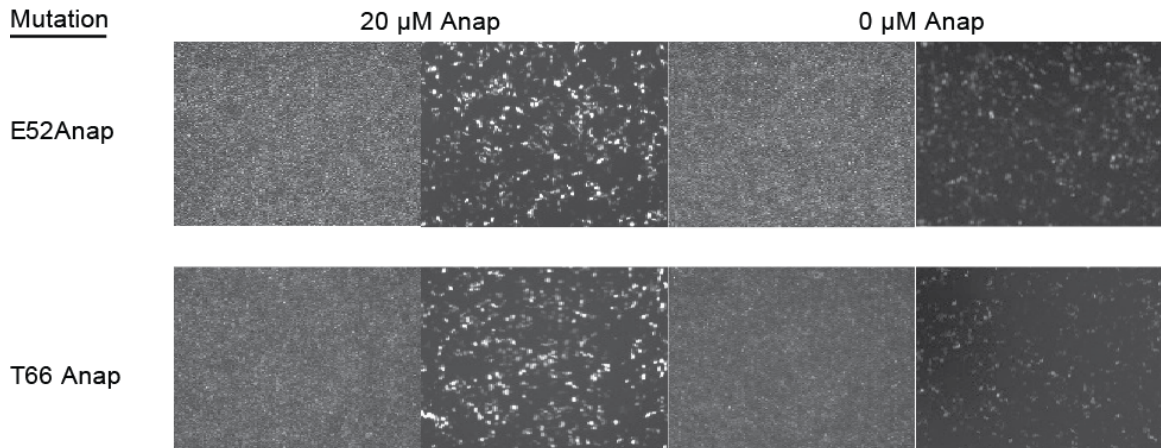
Codon Mutation      Amino Acid Mutation  
**GAA**→TAG              E52Anap

Images of HEK293 cells expressing proteins used in these studies  
EGFP-Y39Anap



SUMO\*-EGFP

Mutation



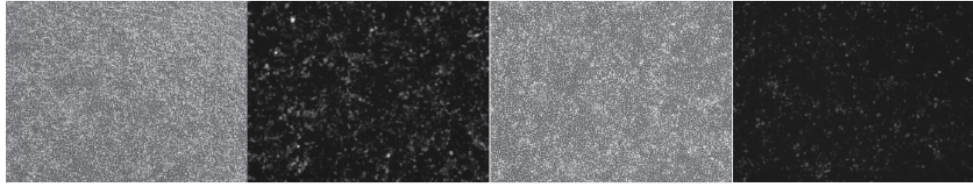
# Cal-M13-EGFP

Mutation

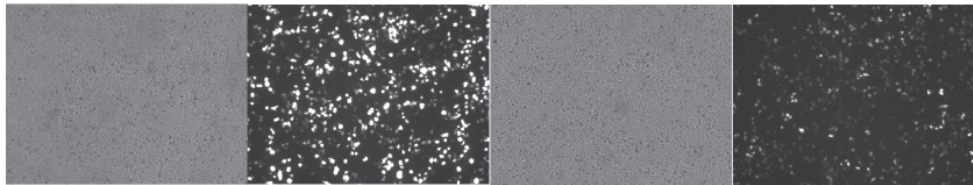
20  $\mu$ M Anap

0  $\mu$ M Anap

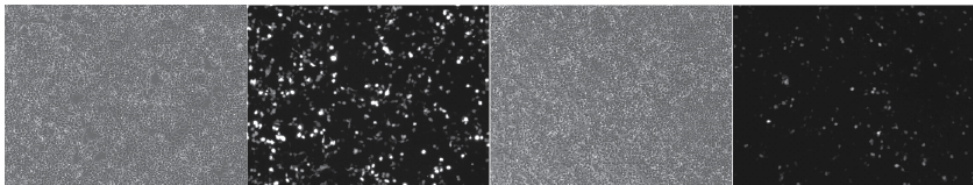
E88Anap



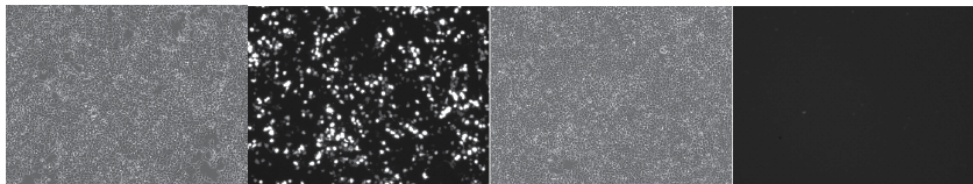
A47Anap



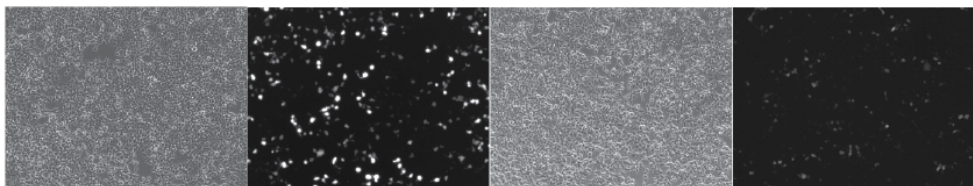
D51Anap



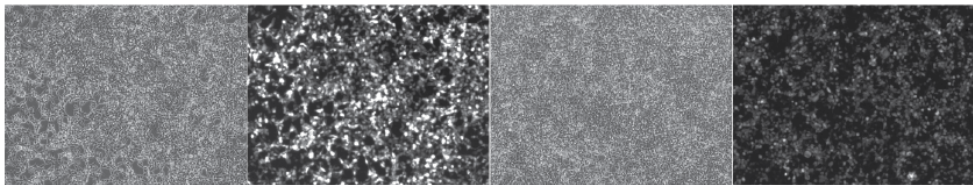
E55Anap



T80Anap



R91Anap



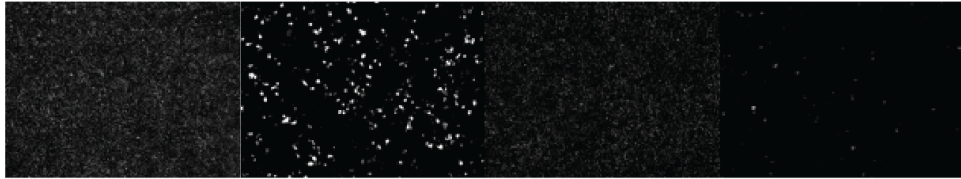
SUMO\*(E52Anap)-YFP

YFP

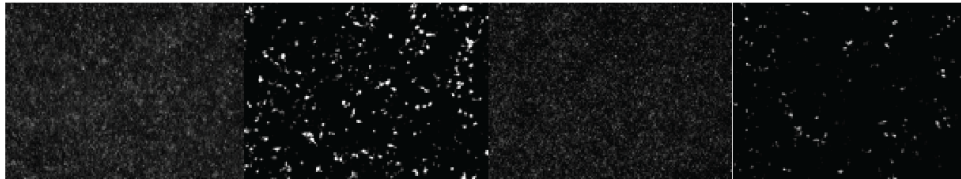
20  $\mu$ M Anap

0  $\mu$ M Anap

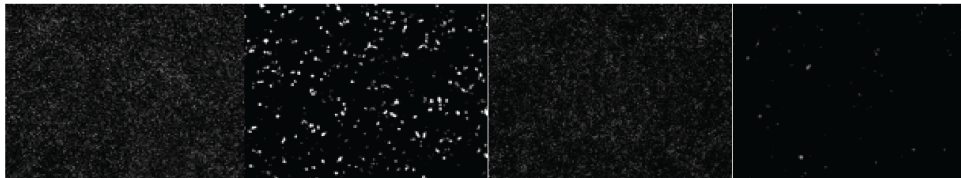
EYFP



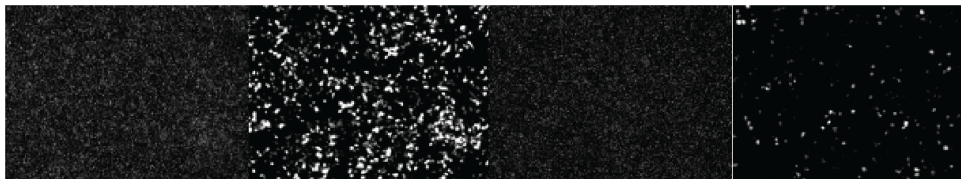
TagYFP



mCitrine



YPet



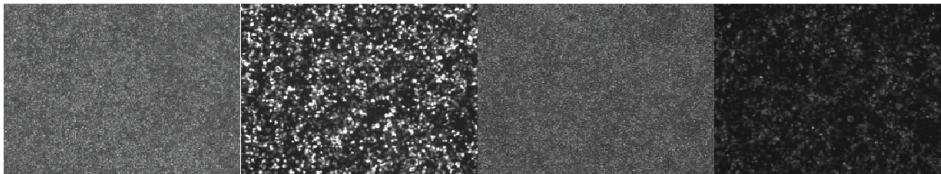
SUMO\*(E52Anap)-DEVD-YFP

YFP

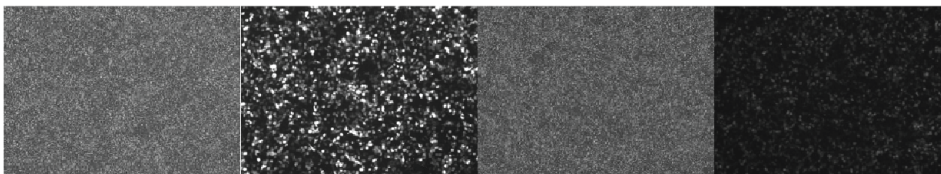
20  $\mu$ M Anap

0  $\mu$ M Anap

TagYFP



YPet

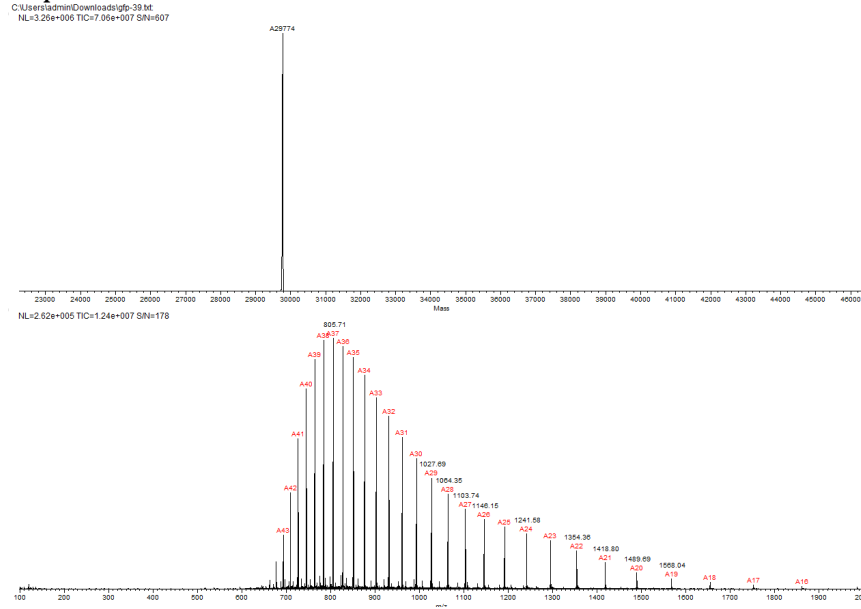


# LC/MS

## EGFP-Y39Anap

Expected mass: 29771

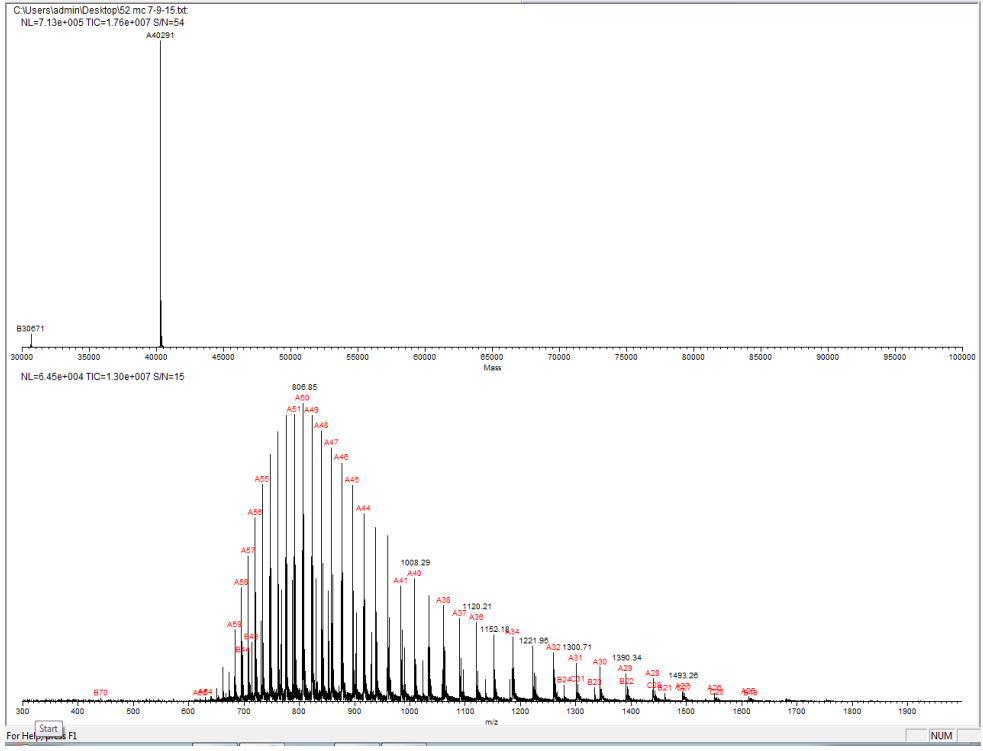
Experimental mass: 29774



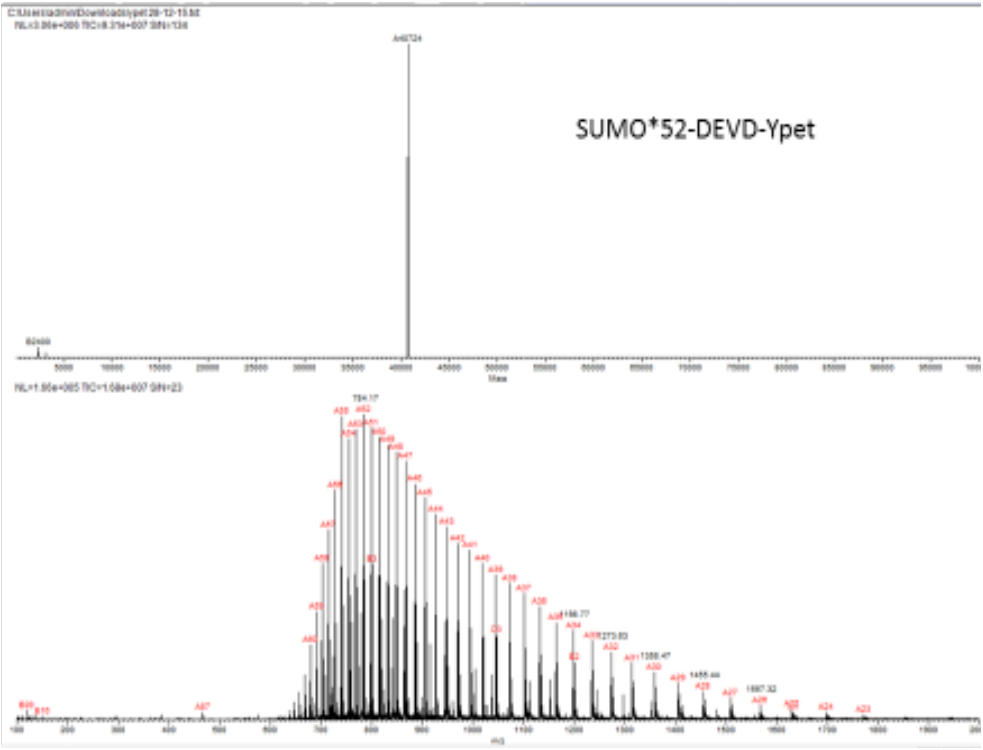




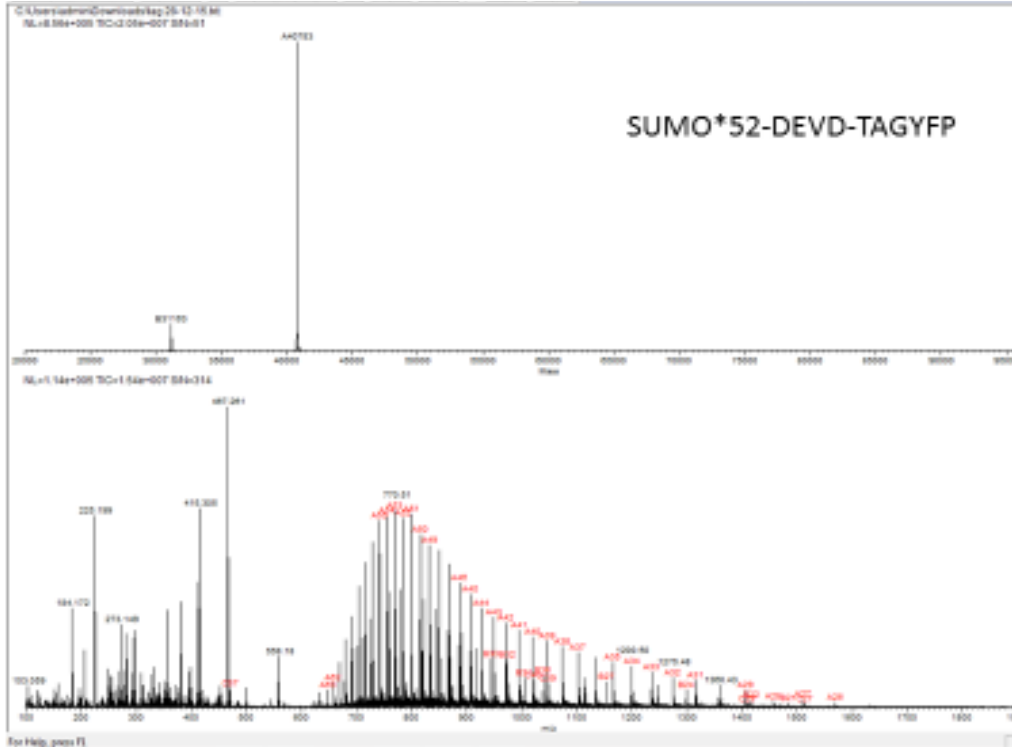
SUMO\*(E52Anap)-mCitrine  
Expected mass: 40293  
Experimental mass: 40291



SUMO\*(E52Anap)-DEVD-Ypet  
Expected mass: 40783  
Experimental mass: 40783



SUMO\*(E52Anap)-DEVD-TagYFP  
Expected mass: 40724  
Experimental mass: 40724



Gel: EGFP-Y39Anap and Cal-M13-EGFP

